Accepted Manuscript

Design, synthesis and biological evaluation of novel naphthoquinone derivatives as IDO1 inhibitors

Liangkun Pan, Qiang Zheng, Yu Chen, Rui Yang, Yanyan Yang, Zhongjun Li, Xiangbao Meng

PII: S0223-5234(18)30671-8

DOI: 10.1016/j.ejmech.2018.08.013

Reference: EJMECH 10624

To appear in: *European Journal of Medicinal Chemistry*

Received Date: 7 April 2018

Revised Date: 7 June 2018

Accepted Date: 4 August 2018

Please cite this article as: L. Pan, Q. Zheng, Y. Chen, R. Yang, Y. Yang, Z. Li, X. Meng, Design, synthesis and biological evaluation of novel naphthoquinone derivatives as IDO1 inhibitors, *European Journal of Medicinal Chemistry* (2018), doi: 10.1016/j.ejmech.2018.08.013.

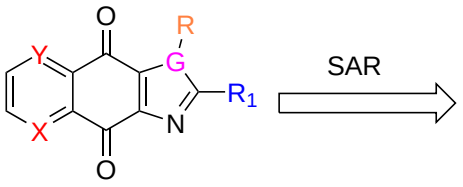

60 naphthoquinone derivatives

SAR

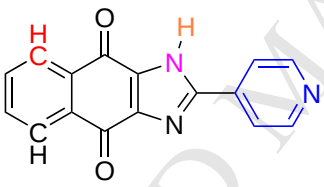

T16

IDO1 IC_{50}=48 nM

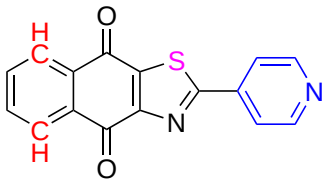

T44

IDO1 IC_{50}=26 nM

IDO1 IC_{50}/TDO IC_{50}

Decrease 50.1% of

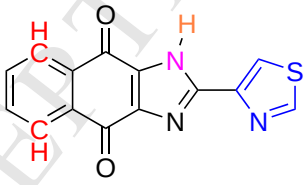

T28

IDO1 IC_{50}=120 nM

TDO IC_{50}=73 nM

Decrease 38.9% of rat KYN

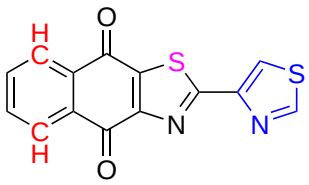

T47

IDO1 IC_{50}=18 nM

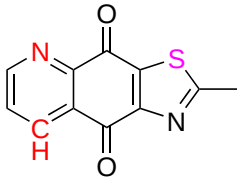

T53

IDO1 IC_{50}=18 nM

IDO1 IC_{50}/TDO IC_{50}

Decrease 30.5% of

Design, synthesis and biological evaluation of novel naphthoquinone derivatives as IDO1 inhibitors

Liangkun Pan, Qiang Zheng, Yu Chen, Rui Yang, Yanyan Yang, Zhongjun Li, Xiangbao Meng*

State Key Laboratory of Natural and Biomimetic Drugs, School of Pharmaceutical Sciences, Peking University, Beijing 100191, China.

*Corresponding author, Email: xbmeng@bjmu.edu.cn

Abstract

Indoleamine 2,3-dioxygenase 1 (IDO1) mediated kynurenine pathway of tryptophan degradation is identified as an appealing and novel target in immunotherapy for the treatment of cancer. In this study, a novel series of naphthoquinone derivatives were synthesized, characterized and evaluated for their inhibitory activities against IDO1, and their structure−activity relationship was investigated. Among them, compounds **T16**, **T44**, **T47**, **T49**, **T53** and **T54** displayed potent IDO1 inhibitory activities with IC_{50} values ranging between 18 and 61 nM, which are more potent than INCB024360 undergoing clinical trial III evaluation. In addition, compounds **T28**, **T44** and **T53** decreased the kynurenine levels in rat plasma by 30% to 50%. Compounds exhibiting excellent IDO1 inhibitory activities were also evaluated for their inhibitory activities against tryptophan 2,3-dioxygenase (TDO). Of which, compound **T28** (IDO1 IC_{50}=120 nM) showed promising TDO inhibition (IC_{50} 72 nM) and was identified as an IDO1/TDO dual inhibitor.

Keywords:

Indoleamine 2,3-dioxygenase 1; cancer immunotherapy; naphthoquinone derivatives; tryptophan 2,3-dioxygenase.

1. Introduction

The interactions between immune system and the development of tumors are dynamic and complex. While the host immune system possesses the capacity of recognizing and destroying tumor cells, many malignancies can develop the capacity to actively suppress a potentially effective immune response and create an immunosuppressive microenvironment to evade

immune destruction with the process of cancer immunoediting [1, 2]. This can be achieved through several molecular mechanisms, including the recruitment of immunosuppressive cells, exclusion of T cells, and activation of immunoinhibitory checkpoint pathways [3]. To date, immunotherapy aiming to breach immune suppressive mechanisms established by tumor cells has become one of the most promising approaches for cancer therapy[4], following operative treatment, chemotherapy, radiotherapy and targeted therapy.

A large body of evidence indicates that the enzyme indoleamine 2,3-dioxygenase 1 (IDO1) plays a critical role in tumor-derived immunosuppression in the tumor microenvironment. It acts by the accumulation of tryptophan metabolites and the depletion of tryptophan. These studies suggest that IDO could be a valid therapeutic target in cancer immunotherapy [5-7]. IDO1 is an extrahepatic cytosolic heme-containing dioxygenase that catalyzes the oxidative cleavage of the C2-C3 double bond of the indole ring in tryptophan to form N-formyl-kynurenine utilizing molecular oxygen or reactive oxygen species via three proposed reaction mechanisms [8, 9]. This reaction is known as the initial and rate limiting step in the kynurenine pathway (KP) of tryptophan catabolism in mammals (**Fig. 1**). The generated *N*-formyl-kynurenine is subsequently metabolized to several active metabolites, including kynurenine, kynurenic acid, 3-hydroxy-kynurenine, quinolinic acid and nicotinamide adenine dinucleotide, which are also known to be involved in a number of neurological disorders, such as Alzheimer's disease, Parkinson's disease, and cerebral ischemia [10].

Figure 1. The kynurenine pathway of tryptophan catabolism in mammals

Many studies have confirmed that IDO1 is suppressed in normal human tissues, including spleen, gut and lung [11, 12], but can be overexpressed by many types of human tumors in a constitutive manner by proinflammatory stimuli such as interferon-γ (IFN-γ) and transforming growth factor-β (TGF-β) [13, 14]. High expression of IDO1 by tumors can lead to the depletion of tryptophan and the accumulation of high levels of kynurenine and its downstream metabolites in the tumor microenvironment. Tryptophan shortage can lead to anergy of

effector T cell via mTORC1 inhibition [15] and GCN2 activation [16], and production of bioactive kynurenine pathway metabolites can result in promotion of Treg differentiation as a consequence of activating the AHR (aryl hydrocarbon receptor) [17]. Over expression of IDO1 also have influence on the conversion of dendritic cell [17] and macrophage [18], the disability of natural killer cell [19] and the production of the reactive oxygen species [20], and thus enabling tumor cells to elude the host immune response.

The identification of IDO1 as a promising therapeutic target prompts extensive searches for its highly active inhibitors. The crystal structures of IDO with the heme-bound ligands cyanide and 4-phenylimidazole (PIM) were reported in 2006 [21], which significantly facilitated the structure-based design of IDO1 inhibitors. Until now, several types of IDO1 inhibitors including indole-analogs (1-MT), quinines derivatives (annulin B, exiguamine A, Aulosirazole), phenyl-imidazole derivatives (NLG919) and hydroxyamidine derivatives (INCB24360) have been reported through structure-based IDO1 inhibitor design, HTS strategy and natural product derivatization **(Fig. 2)**. However, only a few compounds, including indole-analogs d-1MT, hydroxyamidine derivatives INCB24360 and phenyl-imidazole derivatives NLG919, have entered clinical evaluation. There is still an urgent need to discover novel and structurally diverse IDO1 inhibitors.

Figure 2. Structures of representative IDO1 inhibitors

The 1,4-naphthoquinone unit is a privileged scaffold that could be introduced into the structures of potential IDO1 inhibitors [22]. In order to identify more potent IDO1 inhibitors, we designed and synthesized a series of novel 1,4-naphthoquinone derivatives and studied their IDO1 inhibitory activities.

2. Results and discussion

2.1. Chemistry

The synthetic pathways for compounds **T1**-**T43** and **T48**-**T50** (**Table 1**) are depicted in **Scheme 1**. The key intermediate **4** was prepared according to the procedure described in the

literature [23]. Initially, 2,3-dichloronaphthalene-1,4-dione was reacted with potassium phthalimide by refluxing in anhydrous acetonitrile to afford the 2,3-disubstituted naphthoquinone, which was then reduced by hydrazine hydrate to the desired intermediate **4**. Subsequently, intermediate **4** was treated with appropriate aromatic aldehyde in the presence of catalyst sodium pyrosulfite in DMF at 120°C to obtain the corresponding target compound **T1**-**T43** with high yields. 6,7-Dichloroquinoline-5,8-dione (**7**) was obtained by the oxidization of 8-hydroxyquinoline in the presence of oxidant sodium chlorate in concentrated HCl. Target compounds **T48-T50** were synthesized from intermediate **7** following the same route of **T1**-**T43**.

Scheme 1. Reagents and conditions: (a) acetonitrile, reflux, 90%; (b) hydrazine hydrate, water, 65-70°C, 94%; (c) $Na_2S_2O_5$, DMF, 120°C, 70%-90%; (d) NaH, THF, RT, 56%-90%; (e) $NaClO_3$, concentrated hydrochloric acid, 30°C, 29%.

The synthetic route for compounds **T44-T47** and **T51-T54** (**Table 1**) is depicted in **Scheme 2**. Firstly, 2,3-dichloronaphthalene-1,4-dione was reacted with 7M ammonia in methanol to produce monosubstituted intermediate **10**. Next, intermediate **10** was reacted with Na_2S through refluxing in a mixed solution of water and ethanol to form sulfureted intermediate, which was subsequently treated with appropriate aromatic aldehyde in one pot to afford the desired compounds **T44**-**T47**. However, the reaction between intermediate **7** and ammonia could produce two positional isomers intermediate **11a** and **11b**. The mixture was used directly in the condensations with appropriate aromatic aldehyde without further separation. The pure compounds **T51-T54** were separated and purified by silica gel chromatography after the final step. Besides, **T16** and **T25** were treated with appropriate benzyl bromide in THF utilizing NaH as base to give target compounds **T55-T60**.

Scheme 2. Reagents and conditions: (e) 7 N ammonia, methanol, 35°C, 94%; (f) (□) NaS_2, ethanol, water, reflux; (ii) acetic acid, ethanol, water, reflux, 62%-80%.

A total of 60 naphthoquinone derivatives were synthesized (**Table 1**), 45 of which are newly synthesized compounds. All of the new compounds were systematically characterized by melting points, ^{1}H-NMR, ^{13}C-NMR, and HRMS analysis.

Table 1. Structures of naphthoquinone derivatives

2.2 IDO1 Inhibitory Activities

Firstly, 1H-naphtho[2,3-d]imidazole-4,9-dione (**T25)** was chosen as the lead compound. In order to find out the effect of R^1 on the inhibitory activity of IDO1, different substituents were introduced to the C-2 of the imidazole ring of **T25**, including methyl (**T26**), substituted phenyl (**T1-T15**), 4-pyridyl (**T16**), 3-pyridyl (**T17**), 2-pyridyl (**T18**), 5-thiazolyl (**T27**), 4-thiazolyl (**T28**), 4-imidazolyl (**T29**), 4-pyrazolyl (**T30**), 2-thiazolyl (**T31**), 3-pyrryl (**T32**), 2-imidazolyl (**T33**), 3-pyrazolyl (**T34**), 2-pyrryl (**T35**), 2-indolyl (**T36**), 2-thienyl (**T37**), 4-quinolyl (**T42**) and pyrimidinyl (**T43**). All the synthesized compounds were evaluated for their inhibitory activities against IDO1 in comparison with the positive control INCB024360, according to the literature protocol [24]. The results were expressed as inhibitory rate at 1 μM in **Table 2** and the IC_{50} values of some compounds displaying potent inhibitory activity were also presented. Out of these 31 analogs, compound **T16** bearing 4-pyridyl substitution at C-2 of imidazole ring showed the highest inhibitory activity against IDO1 (IC_{50}=48nM) compared to the positive control INCB24360 (IC_{50}=65 nM), whereas the compound with substituted phenyl substitution exhibited moderate inhibitory activity. In addition, compound **T28** with 4-thiazolyl substitution displayed the best inhibitory activity (IC_{50}=120 nM) among all the five-membered rings substituted derivatives, followed by compound **T33** (IC_{50}=134 nM).

Table 2. Inhibitory rate (at 1μM) and IC_{50} (nM) values of the compounds **T1-18**, **T27-37** and **T42-43** derivatives against IDO1

Next, compounds **T16** and **T28** which exhibited the best inhibitory activity in the first round were chosen as parent compounds for further modification. Different substitutions were

introduced to the pyridine ring of **T16** and the thiazole ring of **T28** to search for more potent IDO1 inhibitors. Ten compounds (**T19-T24**, **T38-T41**) were newly synthesized and evaluated for their inhibitory activity against IDO1 at 1 μM. According to the screening results in **Table 3**, the inhibitory activity of all the newly synthesized compounds decreased significantly regardless of substitution and where it was linked, compared with the parent compounds, indicating that further modification at pyridine and thiazole was detrimental to the inhibitory activity of **T16** and **T28**, respectively.

Table 3. Inhibitory rate (at 1μM) and IC_{50} (nM) values of the compounds **T19-24**, **T38-41** derivatives against IDO1

We subsequently tried to modify ring A and ring B of **T16** and **T28** after identifying pyridine and thiazole rings as the optimal substitutions at C-2 of imidazole, respectively. By replacing imidazole with thiazole and (or) replacing C-5 or C-8 of 1,4-naphthoquinone with N atom, 11 new compounds (**T44-54**) were synthesized and evaluated for their inhibitory activities expressed as inhibitory rate (at 1 μM) and IC_{50} value (**Table 4**). The screening results showed that most of the synthesized compounds exhibited potent inhibitory activities against IDO1. The structure-activity-relationships between **T16** and **T44** (or **T28** and **T47**, **T49** and **T53-54**) revealed that the replacements of imidazole with thiazole resulted in an increase of inhibitory activity against IDO1. On the other hand, the introduction of N atom to C-5 or C-8 of 1,4-naphthoquinone might not be beneficial to the improvement of inhibitory activity, judging from the structure-activity-relationships between **T16** and **T48** (or **T44** and **T51-52**, **T28** and **T49**), whereas **T47** and **T53-54** was an exception (**Figure 3A** and **Figure 3B**). Among these 11 analogs, the most promising compounds **T47** and **T53** displayed IC_{50} values of 18 nM against IDO1, more potent than the positive control INCB024360 and the parent compound **T16**, **T28**. In addition, we also introduced substituted benzyl group to N-1 of imidazole of parent compounds **T16** and **T25** to take advantage of the large hydrophobic pocket B in IDO1, leading to another 6 new compounds (**T55-T60**). However, the inhibitory activities of all these compounds bearing benzyl substituents at N-1 of imidazole decreased

dramatically (**Table 4**), implying that N-1 of imidazole might participate in the interactions with the heme iron of IDO1.

Table 4. Inhibitory rates (at 1μM) and IC_{50} (nM) values of the compounds **T44-60** against IDO1

Based on the above inhibitory activity data, a preliminary SAR is summarized in **Figure 3**.

Figure 3. (A)：Structure and inhibitor activity of **T16** derivatives. (B)：Structure and inhibitor activity of **T28** derivatives. (C): Preliminary SAR of synthesized naphthoquinone derivatives.

2.2 TDO Inhibitory Activities

Tryptophan 2,3-dioxygenase (TDO) is another heme containing enzyme mediating the first and rate limiting step of kynurenine pathway of tryptophan degradation, whose tissue distribution and regulation are different from IDO1[25-27]. Recent studies reveal the relationship between TDO and immune escape and implicate TDO in tumor progression, indicating that compounds displaying IDO/TDO dual inhibitory activity may be more desirable in cancer immunotherapy [28, 29]. In light of this, compounds exhibiting promising IDO1 inhibitory activity were tested for their ability to inhibit human TDO, according to the previously described method [30] (**Table 5**). To our delight, the most promising compound **T28** (IDO1 IC_{50}=120 nM) displayed an IC_{50} value of 73 nM against TDO, which is identified as a potent IDO1/TDO dual inhibitor. Besides, other compounds showed great selectivity towards IDO, especially for **T44** (TDO IC_{50}/IDO IC_{50}=61.5) and **T16** (inhibitory rate at 10 μM is 0%). In addition, compounds **T55-T60** which were almost inactive to IDO1 also showed no inhibition against TDO (IC_{50}>100 μM), suggesting the involvement of N-1 of imidazole in the interaction with the heme iron of both IDO1 and TDO.

Table 5. Inhibitory rates and IC_{50} (nM) values of the corresponding compounds against TDO at 10 μM

2.3 Effect of **T28**, **44** and **53** on the reduction of kynurenine levels in rat plasma

The reduction of plasma kynurenine levels is often used as a pharmacodynamic marker for the inhibition of IDO activity. IDO inhibitor **T28**, **T44** and **T53** were selected for further evaluation in vivo. A single intragastric 50 mg/kg dose of corresponding compounds was administered to SD rats. Blood was harvested from individual rat over 8 h. Kynurenine concentrations were measured by enzyme-linked immunosorbent assay kit. Reductions of kynurenine levels by ~30-50% were observed between 0 and 4 h, and kynurenine levels returned to the baseline level after 8 h with maximum inhibition observed at 2h or 4h (**Table 6**). Notably, compound **T44** (IDO IC_{50}= 44 nM) was identified as the most promising compound that could decrease the concentration of kynurenine in rat by 50.1%.

Table 6. T28, **T44** and **T53** suppresses kynurenine generation in vivo[a]

2.4 MTT assay

IDO-1 inhibition assay showed that compound **T16**, **T44**, **T45**, **T47**, **T49**, **T53** and **T54** exhibited better IDO-1 inhibitory activity than the positive control **INCB024360**. The cytotoxic activity of all these compounds and IDO-1/TDO dual inhibitor **T28** were evaluated against human cervical carcinoma cells (HeLa), breast carcinoma cells (MCF-7), and embryonic kidney cells (HEK293T) by MTT assay, using doxorubicin as the positive control. The CC_{50} values of the compounds were represented in **Table 7**. All the compounds displayed an CC_{50} value of micromole level (most CC_{50} values were over 20 μM), which was significantly higher than their IC_{50} values against IDO-1 (showed in **Table 7**). These results reveal that all the promising compounds are not cytotoxic at their effective concentration against IDO-1 (or TDO), and improve their biological importance as cancer immunotherapy agents.

Table 7. Cytotoxic activity of the promising compounds

2.5 LDH cytotoxicity assay

Cell death was evaluated by the quantification of plasma membrane damage which resulted in the release of lactate dehydrogenase (LDH). The level of LDH released in the cell culture supernatant was detected by LDH cytotoxicity assay detection kit (Beyotime, China) following the manufacturer's instructions. The CC_{50} values of the chosen compounds **T16**, **T23**, **T28**, **T33**, **T44**, **T45**, **T47**, **T48**, **T49**, **T50**, **T51**, **T52**, **T53** and **T54** (IDO1 IC_{50}<300 nM) against HeLa and HEK293T at 24h were presented in **Table 7**. According to the results, all these compounds showed no cytotoxity (CC_{50} >40 μM).

3. Conclusion

In conclusion, 60 naphthoquinone derivatives were successfully synthesized and tested for their ability to inhibit human IDO1. The most promising compounds **T47**, **T53, T54** and **T44** displayed IC_{50} values of 18 nM, 18 nM, 22 nM and 26 nM, respectively. Further evaluation in vivo showed that **T28**, **T44** and **T53** reduced kynurenine levels in plasma by 30%-50%. Therefore, dual IDO/TDO inhibitor **T28,** selective IDO1 inhibitors **T44** and **T53** were identified as promising lead compounds and merit further investigation.

4. Experimental

4.1. Chemistry

Unless otherwise noted, all reagents were obtained from commercial suppliers and used without further purification. Reactions were monitored by thin-layer chromatography (TLC) using commercial silica gel HSGF254 plates. Column chromatography was performed on Silica Gel 60 (E. Merck, 230-400 mesh). Melting points were measured on an X-5 micromelting point apparatus and were uncorrected. The ^{1}H-MMR (400 MHz) and ^{13}C-NMR (100.6 MHz) spectra were recorded with BrukerAM-400 spectrometer in $CDCl_3$ and DMSO-d6 solution. Chemical shifts were referenced with tetramethylsilane (TMS). The HR-ESI-MS data were measured on a Bruker Apex IV FTMS.

4.1.1. Procedure for the synthesis of 2,3-Diphthalimido-1,4-naphthoquinone (**3**)

To a solution of 2,3-dichloro-1,4-naphthoquinone (0.02 mol) in anhydrous acetonitrile (100

mL), potassium phthalidimide (0.084 mol), which was previously finely powdered and dried under vacuum, was added. The reaction mixture was refluxed for 3 h, and the hot solution was filtered. The precipitate was washed successively with cold acetonitrile (200 mL), water (200 mL) and methanol (200 mL). 2,3-Diphthalimido-1,4-naphthoquinone was dried under vacuum at 50ºC and isolated as a pale yellow powder (8.02 g) in 90% yield. The characterization data for compound **3** are in accordance with that reported previously[23].

4.1.2. Procedure for the synthesis of 2,3-Diamino-1,4-naphthoquinone (**4**)

To a suspension of 2,3-diphthalimido-1,4-naphthoquinone (5.0 mmol) in water (150 mL) was added a 64% solution in water of hydrazine (20 mL). The solution was stirred for 15 min at room temperature then heated at 65-70°C for 3h. The reaction mixture was allowed to stand at room temperature. The precipitate was filtered, and washed with a large volume of water. Compound **4** was dried overnight under vacuum at 100ºC and isolated as a purple powder (0.88 g) in 94% yield. The characterization data for compound **4** are in accordance with that reported by R. Diaz et al [31].

4.1.3. Procedure for the synthesis of 6,7-dichloroquinoline-5,8-dione (**7**)

Sodium chlorate (0.50 mol) was added over a period of 1 h to a solution of 8-hydroxyquinoline (0.10 mol) in concd HCl (600mL) at 40°C and the reaction mixture stirred for 2 h before being diluted with water to a total volume of 2 L. The white precipitate that formed was removed by filtration and discarded. The filtrate was then extracted with CH_2Cl_2 (6×250mL), the organic phases were combined, washed with water and concentrated in vacuo to give a yellow solid. The solid was then recrystallized in MeOH to yield 7 as bright yellow crystals. The characterization data for compound **7** are in accordance with that reported previously [32].

4.1.4. Procedure for the synthesis of compound **10**, **11a**, **11b**.

To 2,3-dichloro-1,4-naphthoquinone (1.0 mmol) in 1.0 ml of ethanol was added concentrated ammonia (7N in MeOH, 4.0 mmol) and the mixture was stirred at 35°C for 3h. The formed

red precipitate was filtered under suction, washed with distilled water and dried to afford the desired compound as an orange solid, 90%-94.0%. The characterization data for compound **10,11a and 11b** are in accordance with that reported previously[33, 34].

4.1.5. General procedure for the preparation of compounds **T1-T43**.

A solution of 2,3-diamino-1,4-naphthoquinone (1.0mmol), appropriate aromatic aldehyde (1.0 mmol) with sodium pyrosulfite in DMF was stirred at 120 ºC overnight. On completion of the reaction monitored by TLC, the solvent was evaporated and the residue was purified by silica gel chromatography by DCM/MeOH system to afford the final product. If necessary, the crude product could be recrystallized in methanol or DMSO to afford pure sample.

4.1.5.1. 2-(2-Chlorophenyl)-1H-naphtho[2,3-d]imidazole-4,9-dione (**T1**)

Pale yellow solid; yield 80%; m.p. 252-254□; ^{1}H NMR (400 MHz, DMSO-d6) δ 14.37 (s, 1H), 8.10 (dd, J = 6.1, 3.0 Hz, 2H), 7.85 (dd, J = 6.1, 3.0 Hz, 2H), 7.79 (d, J = 7.5Hz, 1H), 7.67 (d, J = 7.5 Hz, 1H), 7.59 (t, J = 7.5 Hz 1H), 7.53 (t, J = 7.5 Hz, 1H); ^{13}C NMR (101 MHz, DMSO) δ 150.83, 134.39, 133.17, 132.65, 132.56, 132.37, 130.72, 129.09, 127.85, 126.80; HR-EI-MS：Calcd for $C_{17}H_9ClN_2O_2$ $[M+H]^+$: 309.0425, found: 309.0416.

4.1.5.2. 2-(3-Chlorophenyl)-1H-naphtho[2,3-d]imidazole-4,9-dione (**T2**)

Brown solid, yield 86%; m.p. >300℃; ^{1}H NMR (400 MHz, DMSO-d6) δ 14.52 (s, 1H), 8.32 (dd, J = 1.7Hz, 1.2 Hz, 1H), 8.21 (ddd, J = 5.0, 3.5, 1.7 Hz, 1H), 8.13 (dd, J = 5.7, 3.3 Hz, 2H), 7.87 (dd, J = 5.7, 3.3 Hz, 2H), 7.63-7.58 (m, 2H); ^{13}C NMR (101 MHz, DMSO) δ 151.18, 134.32, 134.24, 133.15, 131.36, 130.92, 130.65, 126.78, 126.73, 125.78. HR-ESI-MS: Calcd for $C_{17}H_9ClN_2O_2$ $[M+H]^+$: 309.0425, found: 309.0411.

4.1.5.3. 2-(4-Chlorophenyl)-1H-naphtho[2,3-d]imidazole-4,9-dione (**T3**)

Pale yellow solid; yield 80%; m.p. 300-302℃; ^{1}H NMR (400 MHz, DMSO-d6) δ 14.45 (s, 1H), 8.23 (d, J = 8.3 Hz, 2H), 8.09 (dd, J = 5.7, 3.3 Hz, 2H), 7.84 (dd, J = 5.8, 3.3 Hz, 2H), 7.62 (d, J = 8.4 Hz, 2H). Other characterization data are in accordance with that reported

previously[35].

4.1.5.4. 2-(2-Fluorophenyl)-1H-naphtho[2,3-d]imidazole-4,9-dione (**T4**)

Pale yellow solid; yield 76%; m.p. >300□; ^{1}H NMR (400 MHz, DMSO-d6) δ 14.27 (s, 1H), 8.12 (dd, J = 5.9, 3.0 Hz, 2H), 8.01 (t, J = 7.7 Hz, 2H), 7.87 (dd, J = 5.8, 3.0 Hz, 2H), 7.62 (q, J = 7.2 Hz, 2H), 7.49-7.34 (m, 2H). Other characterization data are in accordance with that reported previously[36].

4.1.5.5. 2-(4-Fluorophenyl)-1H-naphtho[2,3-d]imidazole-4,9-dione (**T5**)

Pale yellow solid; yield 80%; m.p. >300□; ^{1}H NMR (400 MHz, DMSO-d6) δ 14.37 (s, 1H), 8.28 (t, J = 6.4 Hz, 2H), 8.10 (dd, J = 6.1, 3.3 Hz, 2H), 7.85 (dd, J = 6.1, 3.3 Hz, 2H), 7.40 (t, J = 9.1 Hz, 1H). Other characterization data are in accordance with that reported previously[35].

4.1.5.6. 2-(2-Bromophenyl)-1H-naphtho[2,3-d]imidazole-4,9-dione (**T6**)

Pale yellow solid; yield 89%; m.p. 245-247□; ^{1}H NMR (400 MHz, DMSO-d6) δ 14.39 (s, 1H), 8.12 (dd, J = 5.7, 3.2 Hz, 2H), 7.91-7.79 (m, 3H), 7.71 (d, J = 7.7 Hz, 1H), 7.57 (t, J = 7.7 Hz, 1H), 7.51 (t, J = 7.7 Hz, 1H). 13C NMR (101 MHz, DMSO) δ 152.10, 134.43, 133.80, 133.19, 132.67, 132.51, 131.33, 128.27, 126.80, 122.37. HR-ESI-MS: Calcd for $C_{17}H_9BrN_2O_2$ $[M+H]^+$:352.9920, found:352.9914.

4.1.5.7. 2-(2-Methoxyphenyl)-1H-naphtho[2,3-d]imidazole-4,9-dione (**T7**)

Pale yellow solid; yield 90%; m.p. 264-266□; ^{1}H NMR (400 MHz, DMSO-d6) δ 13.40 (s, 1H), 8.09 (dd, J = 5.7, 3.3 Hz, 2H), 7.97 (dd, J = 7.7, 1.8 Hz, 1H), 7.84 (dd, J = 5.7, 3.3 Hz, 2H), 7.52 (ddd, J = 8.3, 7.7, 1.8 Hz, 1H), 7.22 (d, J = 8.3 Hz, 1H), 7.11 (td, J = 7.7, 1.0 Hz, 1H), 3.94 (s, 3H). ^{13}C NMR (101 MHz, DMSO) δ 157.38, 150.77, 134.26, 133.23, 132.60, 130.92, 126.71, 121.10, 117.76, 112.29, 56.19. HR-ESI-MS: Calcd for $C_{18}H_{12}N_2O_3$ $[M+H]^+$: 305.0921, found: 305.0913.

4.1.5.8. 2-(3-Methoxyphenyl)-1H-naphtho[2,3-d]imidazole-4,9-dione (**T8**)

Pale yellow solid; yield 89%; m.p. 310□; ^{1}H NMR (400 MHz, DMSO-d6) δ 14.29 (s, 1H), 8.06 (dd, J = 5.7, 3.3 Hz, 2H), 7.86 – 7.70 (m, 4H), 7.41 (t, J = 8.0 Hz, 1H), 7.02 (d, J = 8.2 Hz, 1H), 3.84 (s, 3H). ^{13}C NMR (101 MHz, DMSO) δ 159.98, 152.60, 134.31, 133.18, 130.53, 130.17, 126.72, 119.60, 117.36, 111.67, 55.77. HR-ESI-MS: Calcd for $C_{18}H_{12}N_2O_3$ $[M+H]^+$: 305.0921, found:305.0910.

4.1.5.9. 2-(4-Methoxyphenyl)-1H-naphtho[2,3-d]imidazole-4,9-dione (**T9**)

Reddish brown solid; m.p. 320-322□; yield 86; ^{1}H NMR (400 MHz, DMSO-d6) δ 14.16 (s, 1H), 8.19 (d, J = 8.8 Hz, 2H), 8.09 (dd, J = 5.7, 3.3 Hz, 2H), 7.84 (dd, J = 5.7, 3.3 Hz, 2H), 7.10 (d, J = 8.8 Hz, 2H), 3.84 (s, 3H). Other characterization data are in accordance with that reported previously[35].

4.1.5.10. 3-(4,9-Dioxo-4,9-dihydro-1H-naphtho[2,3-d]imidazol-2-yl)benzonitrile (**T10**)

Orange solid; yield 74%; m.p. >300□; ^{1}H NMR (400 MHz, DMSO-d6) δ 14.45 (s, 1H), 8.51 (s, 1H), 8.43 (d, J = 8.0 Hz, 1H), 8.02 (dd, J = 5.7, 3.3 Hz, 2H), 7.90 (d, J = 7.7 Hz, 1H), 7.79 (dd, J = 5.7, 3.3 Hz, 2H), 7.70 (t, J = 7.9 Hz, 1H). ^{13}C NMR (101 MHz, DMSO) δ 150.53, 134.31, 134.07, 133.07, 131.52, 130.73, 130.45, 130.03, 126.72, 118.61, 112.59. HR-ESI-MS: Calcd for $C_{18}H_9N_3O_2$ $[M+H]^+$: 300.0768, found: 300.0768.

4.1.5.11. 4-(4,9-Dioxo-4,9-dihydro-1H-naphtho[2,3-d]imidazol-2-yl)benzonitrile (**T11**)

Yellow solid; yield 80%; m.p. >300□; ^{1}H NMR (400 MHz, DMSO-d6) δ 14.60 (s, 1H), 8.45-8.22 (m, 2H), 8.19 -7.67 (m, 6H).^{13}C NMR (101 MHz, DMSO) δ 181.15, 154.49, 141.66, 135.48, 134.45, 133.44, 133.29, 132.96, 131.29, 127.81, 127.53, 126.83, 118.89, 112.97. HR-ESI-MS: Calcd for $C_{18}H_9N_3O_2$ $[M+H]^+$: 300.0768, found: 300.0766.

4.1.5.12. Methyl 4-(4,9-dioxo-4,9-dihydro-1H-naphtho[2,3-d]imidazol-2-yl) benzoate (**T12**)

Brown solid; yield 88%; m.p. >300□; ^{1}H NMR (400 MHz, DMSO-d6) δ 14.45 (s, 1H), 8.26 (d, J = 8.0 Hz, 2H), 8.04 (dd, J = 5.7, 3.3 Hz, 2H), 7.98 (d, J = 8.1 Hz, 2H), 7.80 (dd, J = 5.8,

3.3 Hz, 2H), 3.84 (s, 1H). ^{13}C NMR (101 MHz, DMSO) δ 198.67, 165.96, 151.38, 134.40, 133.14, 131.11, 130.23, 127.49, 127.31, 126.70, 55.36. HR-ESI-MS: Calcd for $C_{19}H_{12}N_2O_4$ $[M+H]^+$: 333.0870, found: 333.0893.

4.1.5.13. 4-(4,9-Dioxo-4,9-dihydro-1H-naphtho[2,3-d]imidazol-2-yl)benzoic acid (**T13**)

Yellow solid; yield 94%。m.p. >300□; ^{1}H NMR (400 MHz, DMSO-d6) δ 13.75 (br s, 1H), 8.33 (d, J = 8.1 Hz, 2H), 8.13-8.00 (m, 4H), 7.84 (dd, J = 5.7, 3.3 Hz, 2H). ^{13}C NMR (101 MHz, DMSO) δ 177.36, 167.18, 151.83, 134.29, 133.23, 132.82, 132.54, 130.25, 127.28, 126.73. HR-ESI-MS: Calcd for $C_{18}H_{10}N_2O_4$ $[M+H]^+$: 309.0425, found: 309.0416.

4.1.5.14. 2-(4-Nitrophenyl)-1H-naphtho[2,3-d]imidazole-4,9-dione (**T14**)

Yellow solid; yield 90%; m.p. >300□; ^{1}H NMR (400 MHz, DMSO-d6) δ 8.42 (m, 2H), 8.33 (s, 2H), 8.07 (s, 2H), 7.08 (s, 2H). Other characterization data are in accordance with that reported previously[37].

4.1.5.15. 2-(3-Nitrophenyl)-1H-naphtho[2,3-d]imidazole-4,9-dione (**T15**)

Yellow solid; yield 86%; m.p. >300□; ^{1}H NMR (400 MHz, DMSO-d6) δ 9.02 (s, 1H), 8.58 (d, J=7.9Hz, 2H), 8.25 (dd, J=16.9, 8.7Hz, 3H), 8.05 (s, 2H), 7.91 (d, J=16.2Hz, 1H). ^{13}C NMR (101 MHz, DMSO) δ 188.82, 177.23, 150.99, 148.80, 148.63, 141.22, 136.97, 134.90, 134.25, 133.24, 133.12, 131.06, 130.92, 128.31, 126.70, 125.15, 125.00, 123.33, 121.63. HR-ESI-MS: Calcd for $C_{17}H_9N_3O_4$ $[M+H]^+$: 318.0520, found: 318.0533.

4.1.5.16. 2-(Pyridin-4-yl)-1H-naphtho[2,3-d]imidazole-4,9-dione (**T16**)

Yellow solid; yield 74%; m.p. >300□; ^{1}H NMR (400 MHz, CF_3COOD) δ 8.78(d, J=6.4Hz, 2H), 8.55(d, J=6.4Hz, 2H), 8.07 (dd, J=5.0, 3.7Hz, 2H), 7.65 (dd, J=5.1Hz, 3.7Hz, 2H). ^{13}C NMR (101 MHz, CF_3COOD) δ 180.73, 145.94, 144.62, 141.43, 137.99, 134.23, 130.32, 126.71. Other characterization data are in accordance with that reported previously[35].

4.1.5.17. 2-(Pyridin-3-yl)-1H-naphtho[2,3-d]imidazole-4,9-dione (**T17**)

Yellow solid; yield 76%; m.p. >300□; ^{1}H NMR (400 MHz, DMSO-d6) δ 14.61 (s, 1H), 9.38 (d, J = 2.1 Hz, 1H), 8.72 (dd, J = 4.8, 2.1 Hz, 1H), 8.60-8.51 (m, 1H), 8.13 (dd, J = 5.7, 3.4 Hz, 2H), 7.88 (dd, J = 5.7, 3.4Hz, 2H), 7.61 (dd, J = 8.1, 4.8 Hz, 1H). ^{13}C NMR (101 MHz, DMSO) δ 151.51, 150.43, 148.17, 134.57, 134.38, 133.17, 126.78, 125.17, 124.41. HR-ESI-MS: Calcd for $C_{16}H_9N_3O_2$ $[M+H]^+$: 276.0768, found: 276.0758.

4.1.5.18. 2-(Pyridin-2-yl)-1H-naphtho[2,3-d]imidazole-4,9-dione (**T18**)

Brown solid; yield 70%; m.p. >300□; ^{1}H NMR (400 MHz, DMSO-d6) δ 14.69 (br.s, 1H), 8.76 (d, J = 4.8 Hz, 1H), 8.29 (d, J = 7.9 Hz, 1H), 8.12 (dd, J = 5.7, 3.4 Hz, 2H), 8.04 (td, J = 7.9, 1.5 Hz, 1H), 7.87 (dd, J = 5.7, 3.4 Hz, 2H), 7.62-7.49 (m, 1H). Other characterization data are in accordance with that reported previously[37].

4.1.5.19. 2-(3-Fluoropyridin-4-yl)-1H-naphtho[2,3-d]imidazole-4,9-dione (**T19**)

Yellow solid; yield 80%; m.p. >300□; ^{1}H NMR (400 MHz, DMSO-d6) δ 14.66 (s, 1H), 8.83 (s, 1H), 8.63 (d, J = 5.0 Hz, 1H), 8.13 (dd, J = 6.2, 3.1 Hz, 2H), 8.06 (t, J = 5.8 Hz, 1H), 7.88 (dd, J = 6.2, 3.1 Hz, 2H). ^{13}C NMR (101 MHz, DMSO) δ 157.16, 154.54, 146.81, 145.90, 140.09, 139.86, 134.49, 133.19, 126.87, 124.33, 123.77. HR-ESI-MS: Calcd for $C_{16}H_8FN_3O_2$ $[M+H]^+$: 294.0673, found: 294.0664.

4.1.5.20. 2-(2-Methoxypyridin-4-yl)-1H-naphtho[2,3-d]imidazole-4,9-dione (**T20**)

Yellow solid; yield 82%; m.p. >300□; ^{1}H NMR (400 MHz, DMSO-d6) δ 14.67 (s, 1H), 8.33 (d, J = 5.3 Hz, 1H), 8.11 (dd, J = 5.7, 3.4 Hz, 2H), 7.86 (dd, J = 5.7, 3.3 Hz, 2H), 7.74 (d, J = 5.3 Hz, 1H), 7.58 (s, 1H), 3.91 (s, 3H). ^{13}C NMR (101 MHz, DMSO) δ 164.76, 150.10, 148.46, 138.92, 134.44, 133.21, 126.81, 114.53, 107.66, 54.00. HR-ESI-MS: Calcd for $C_{17}H_{11}N_3O_3$ $[M+H]^+$: 306.0873, found: 306.0878.

4.1.5.21. Procedure for the synthesis of 2-(2-hydroxypyridin-4-yl)-1H-naphtho[2,3-d] imidazole-4,9-dione (**T21**)

A solution of T20 (1mmol) in DMF (2ml) was treated with lithium chloride (5mmol) and

pTSA (5mmol), heated at 120 ºC for 30 min, cooled to room temperature, quenched with water (5ml), and extracted with ethyl acetate (2 × 5ml). The combined extracts were washed with water (2 × 5ml) and saturated aqueous brine (2 × 5ml), dried (Na_2SO_4), and concentrated in vacuo to give the desired products **T21** in 99% yield. Pale yellow solid; yield 98%; m.p. >300□; ^{1}H NMR (400 MHz, DMSO-d6) δ 14.61 (s, 1H), 11.82 (s, 1H), 8.12 (dd, J = 5.7, 3.4 Hz, 2H), 7.87 (dd, J = 5.7, 3.3 Hz, 2H), 7.54 (d, J = 6.9 Hz, 1H), 7.20 (s, 1H), 6.94 (d, J = 6.8 Hz, 1H). ^{13}C NMR (101 MHz, DMSO-d6) δ 162.68, 149.98, 140.30, 136.76, 134.40, 133.20, 126.80, 117.61, 102.92. HR-ESI-MS: Calcd for $C_{16}H_9N_3O_3$ $[M+H]^+$: 292.0717, found: 292.0702.

4.1.5.22. 2-(3-Chloropyridin-4-yl)-1H-naphtho[2,3-d]imidazole-4,9-dione (**T22**)

Brown solid; yield 84%; m.p. 286□; ^{1}H NMR (400 MHz, DMSO-d6) δ 14.67 (s, 1H), 8.86 (s, 1H), 8.71 (d, J = 5.0 Hz, 1H), 8.09 (dd, J = 5.7, 3.4 Hz, 2H), 7.92 – 7.77 (m, 3H). ^{13}C NMR (101 MHz, DMSO-d6) δ 150.82, 148.80, 148.19, 135.65, 134.49, 133.14, 129.62, 126.87, 125.69. HR-ESI-MS: Calcd for $C_{16}H_8ClN_3O_2$ $[M+H]^+$: 310.0378, found: 310.0368.

4.1.5.23. 2-(2-Chloropyridin-4-yl)-1H-naphtho[2,3-d]imidazole-4,9-dione (**T23**)

Yellow solid; yield 72%; m.p. >300□; ^{1}H NMR (400 MHz, DMSO-d6) δ 14.86 (s, 1H), 8.61 (d, J = 5.2 Hz, 1H), 8.28 (d, J = 1.4 Hz, 1H), 8.17 (dd, J = 5.2, 1.5 Hz, 1H), 8.14 (dd, J = 5.7, 3.3 Hz, 2H), 7.88 (dd, J = 5.7, 3.3 Hz, 2H). ^{13}C NMR (101 MHz, DMSO-d6) δ 151.81, 151.41, 148.76, 139.56, 139.27, 134.70, 133.05, 126.74, 120.96, 120.20. HR-ESI-MS: Calcd for $C_{16}H_8ClN_3O_2$ $[M+H]^+$: 308.0232, found: 308.0242.

4.1.5.24. 4-(4,9-Dioxo-4,9-dihydro-1H-naphtho[2,3-d]imidazol-2-yl)pyridine 1-oxide (**T24**)

To a stirred solution of T16 (5 mmol) in $CHCl_3$ (2 mL) was added 70% m-CPBA (5 mmol), portion wise at 0 ºC. The resulting mixture was stirred at room temperature for 12 h, at which time complete consumption of starting material was observed by TLC. The reaction mixture was diluted with $CHCl_3$, and solid K_2CO_3 (4mol) was added. The resulting mixture was stirred for an additional 10 min. The solid was separated by filtration, and the filtrate was

dried over Na_2SO_4 and concentrated under reduced pressure to afford the T24. Yellow solid; yield 60%; m.p. >300□; ^{1}H NMR (400 MHz, DMSO-d6) δ 14.61 (s, 1H), 8.36 (d, J = 6.4 Hz, 2H), 8.16 (d, J = 6.4 Hz, 2H), 8.10 (dd, J = 5.8, 3.3 Hz, 2H), 7.85 (dd, J = 5.8, 3.3 Hz, 2H). ^{13}C NMR (101 MHz, DMSO-d6) δ 177.42, 150.16, 139.76, 134.31, 133.32, 126.73, 125.60, 124.08. HR-ESI-MS: Calcd for $C_{16}H_9N_3O_3$ $[M+H]^+$: 290.0571, found: 290.0565.

4.1.5.25. 1H-Naphtho[2,3-d]imidazole-4,9-dione (**T25**)

T25 was synthesized using the approach reported previously [38]. A mixture of 2,3-diamino -1,4-naphthoquinone (79.7mmol) and 25 mL of formic acid (97%) in distilled water (100mL) was refluxed with stirring for 5 h. After cooling to room temperature, the pH of the solution was adjusted to 9 with the addition of 30% ammonium hydroxide. The dark yellow powder (T25) was obtained in yield of 83% after repeated filtration and washing with distilled water. The product was recrystallized from DMSO for further purification. Dark yellow solid; yield 83%; m.p. 369□; ^{1}H NMR (400 MHz, DMSO-d6) δ 14.11 (s, 1H), 8.30 (s, 1H), 8.09 (dd, J = 5.7, 3.3 Hz, 2H), 7.85 (dd, J = 5.7, 3.3 Hz, 2H). Other characterization data are in accordance with that reported previously[38].

4.1.5.26. 2-Methyl-1H-naphtho[2,3-d]imidazole-4,9-dione (**T26**)

A solution of 2,3-Diamino-1,4-naphthoquinone (1mmol) in glacial acetic acid (30mL) was heated at reflux for 7 h. The reaction mixture was cooled and the precipitate obtained was filtered and washed with acetic acid. The product obtained was dissolved in acetone (5mL) and applied on PLC by silica gel (Toluene: ethyl acetate:10:1) as reported previously [39]. The product was recrystallized from ethanol to give gray crystals, yield 70%; m.p. 350□; ^{1}H NMR (400 MHz, DMSO-d6) δ 13.73 (s, 1H), 8.05 (dd, J = 5.8, 3.1 Hz, 2H), 7.82 (dd, J = 5.8, 3.1 Hz, 2H), 2.45 (s, 3H). Other characterization data are in accordance with that reported previously[39].

4.1.5.27. 2-(Thiazol-5-yl)-1H-naphtho[2,3-d]imidazole-4,9-dione (**T27**)

Brown solid; yield 78%; m.p. >200□; ^{1}H NMR (400 MHz, DMSO-d6) δ 14.59 (s, 1H), 9.25 (s, 1H), 8.67 (s, 1H), 8.05 (dd, J = 6.1, 3.0 Hz, 2H), 7.81 (dd, J = 6.1, 3.0 Hz, 2H). 13C NMR (101 MHz, DMSO-d6) δ 157.52, 146.04, 143.62, 134.35, 133.07, 128.33, 126.73. HR-ESI-MS: Calcd for $C_{14}H_7N_3O_2S$ $[M+H]^+$: 280.0186, found: 280.0179.

4.1.5.28. 2-(Thiazol-4-yl)-1H-naphtho[2,3-d]imidazole-4,9-dione (**T28**)

Brown solid; yield 80%; m.p. >300□; ^{1}H NMR (400 MHz, DMSO-d6) δ 14.56 (s, 1H), 9.34 (d, J = 1.9 Hz, 1H), 8.58 (d, J = 1.9 Hz, 1H), 8.11 (dd, J = 5.7, 3.4 Hz, 2H), 7.86 (dd, J = 5.8, 3.3 Hz, 2H). 13C NMR (101 MHz, DMSO-d6) δ 156.29, 148.54, 145.93, 134.27, 133.25, 126.69, 121.93.

HR-ESI-MS: Calcd for $C_{14}H_7N_3O_2S$ $[M+H]^+$:282.0332, found: 282.0325.

4.1.5.29. 2-(1H-imidazol-4-yl)-1H-naphtho[2,3-d]imidazole-4,9-dione (**T29**)

Reddish brown solid; yield 75%; m.p. >300□; ^{1}H NMR (400 MHz, DMSO-d6) δ 8.08 (dd, J = 5.7, 3.3 Hz, 2H), 7.95 (s, 2H), 7.84 (dd, J = 5.6, 3.3 Hz, 2H). 13C NMR (101 MHz, DMSO-d6) δ 177.22, 149.23, 137.72, 134.14, 133.22, 126.57, 121.04. HR-ESI-MS: Calcd for $C_{14}H_8N_4O_2$ $[M+H]^+$:265.0720, found: 265.0713.

4.1.5.30. 2-(1H-pyrazol-4-yl)-1H-naphtho[2,3-d]imidazole-4,9-dione (**T30**)

Brown solid; yield 70%; m.p. >300□; ^{1}H NMR (400 MHz, DMSO-d6) δ 14.01 (s, 1H), 13.29 (s, 1H), 8.36 (s, 2H), 8.09 (dd, J = 5.7, 3.3 Hz, 2H), 7.85 (dd, J = 5.7, 3.3 Hz, 2H). ^{13}C NMR (101 MHz, DMSO-d6) δ 179.01, 175.39, 162.79, 148.50, 143.81, 134.50, 134.07, 133.00, 126.82, 126.33, 111.90. HR-ESI-MS: Calcd for $C_{14}H_8N_4O_2$ $[M+H]^+$:265.0720, found: 265.0705.

4.1.5.31. 2-(Thiazol-2-yl)-1H-naphtho[2,3-d]imidazole-4,9-dione (**T31**)

Tan solid; yield 68%; m.p. >300□; ^{1}H NMR (400 MHz, DMSO-d6) δ 15.06 (s, 1H), 8.16 – 8.08 (m, 3H), 8.06 (d, J = 3.1 Hz, 1H), 7.78 (dd, J = 5.7, 3.3 Hz, 2H). ^{13}C NMR (101 MHz,

DMSO-d6) δ 157.28, 147.30, 145.11, 144.93, 134.43, 133.27, 126.81, 124.34. HR-ESI-MS: Calcd for $C_{14}H_7N_3O_2S$ $[M+H]^+$: 282.0332, found: 282.0324.

4.1.5.32. 2-(1H-pyrrol-3-yl)-1H-naphtho[2,3-d]imidazole-4,9-dione (**T32**)

Purple solid; yield 74%; m.p. >300□; ^{1}H NMR (400 MHz, DMSO-d6) δ 13.72 (s, 1H), 11.37 (s, 1H), 8.12 – 8.05 (dd, J = 5.8, 3.3 Hz, 2H), 7.83 (dd, J = 5.8, 3.3 Hz, 2H), 7.67 (s, 1H), 6.92 (d, J = 2.7 Hz, 1H), 6.81 (s, 1H). ^{13}C NMR (101 MHz, DMSO-d6) δ 179.18, 175.21, 151.65, 143.97, 134.03, 133.18, 126.69, 126.27, 120.02, 113.42, 107.44. HR-ESI-MS: Calcd for $C_{15}H_9N_3O_2$ $[M+H]^+$: 286.0587, found: 286.0582.

4.1.5.33. 2-(1H-imidazol-2-yl)-1H-naphtho[2,3-d]imidazole-4,9-dione (**T33**)

Brown solid; yield 80%; m.p. >300□; ^{1}H NMR (400 MHz, DMSO-d6) δ 8.11 (dd, J = 5.7, 3.3 Hz, 2H), 7.86 (dd, J = 5.7, 3.3 Hz, 2H), 7.39 (s, 2H). ^{13}C NMR (101 MHz, DMSO-d6) δ 177.80, 146.28, 141.23, 138.50, 134.16, 133.59, 126.66, 124.13. HR-ESI-MS: Calcd for $C_{14}H_8N_4O_2$ $[M+H]^+$: 265.0720, found: 265.0714.

4.1.5.34. 2-(1H-pyrazol-3-yl)-1H-naphtho[2,3-d]imidazole-4,9-dione (**T34**)

Tan solid; yield 65%; m.p. >300□; ^{1}H NMR (400 MHz, DMSO-d6) δ 14.36 (s, 1H), 13.47 (s, 1H), 8.15 – 8.04 (m, 2H), 7.96 (s, 1H), 7.85 (dd, J = 5.7, 3.3 Hz, 2H), 7.02 (s, 1H). ^{13}C NMR (101 MHz, DMSO-d6) δ 179.12, 175.64, 148.88, 143.88, 142.12, 134.86, 134.29, 133.28, 130.84, 126.79, 105.49. HR-ESI-MS: Calcd for $C_{14}H_8N_4O_2$ $[M+Na]^+$: 287.0539, found: 287.0525.

4.1.5.35. 2-(1H-pyrrol-2-yl)-1H-naphtho[2,3-d]imidazole-4,9-dione (**T35**)

Purple solid; yield 68%; m.p. >300□; ^{1}H NMR (400 MHz, DMSO-d6) δ 13.92 (s, 1H), 11.99 (s, 1H), 8.08 (dd, J = 5.7, 3.2 Hz, 2H), 7.83 (dd, J = 5.7, 3.3 Hz, 2H), 7.09 (d, J = 2.0 Hz, 1H), 7.00 (s, 1H), 6.34 – 6.16 (m, 1H). ^{13}C NMR (101 MHz, DMSO-d6) δ 179.09, 175.34, 148.22, 143.82, 134.16, 133.22, 126.70, 126.38, 122.96, 121.50, 111.24, 110.08. HR-ESI-MS: Calcd for $C_{15}H_9N_3O_2$ $[M+H]^+$: 262.0622, found: 262.0633.

4.1.5.36. 2-(1H-indol-2-yl)-1H-naphtho[2,3-d]imidazole-4,9-dione (**T36**)

Tan solid; yield 67%; m.p. >300□; ^{1}H NMR (400 MHz, DMSO-d6) δ 14.48 (s, 1H), 12.15 (s, 1H), 8.13 (dd, J = 5.8, 3.1 Hz, 2H), 7.88 (dd, J = 5.8, 3.1 Hz, 2H), 7.66 (d, J = 8.0 Hz, 1H), 7.49 (d, J = 8.2 Hz, 1H), 7.43 (d, J = 2.0 Hz, 1H), 7.22 (t, J = 7.6 Hz, 1H), 7.08 (t, J = 7.5 Hz, 1H). ^{13}C NMR (101 MHz, DMSO-d6) δ 181.40, 162.83, 147.63, 137.91, 134.33, 133.28, 128.15, 127.33, 126.72, 123.78, 121.56, 120.41, 112.64, 103.48.133.27, 126.81, 124.34. HR-ESI-MS: Calcd for $C_{19}H_{11}N_3O_2$ $[M+H]^+$: 312.0779, found: 312.0769.

4.1.5.37. 2-(Thiophen-2-yl)-1H-naphtho[2,3-d]imidazole-4,9-dione (**T37**)

Yellow solid; yield 68%; m.p. >300□; ^{1}H NMR (400 MHz, DMSO-d6) δ 14.45 (s, 1H), 8.10 (dd, J = 5.6, 3.3 Hz, 2H), 8.03 (d, J = 3.6 Hz, 1H), 7.86 (dd, J = 5.9, 3.4 Hz, 2H), 7.83 (d, J = 5.1 Hz, 1H), 7.26 (t, J = 4.3 Hz, 1H). ^{13}C NMR (101 MHz, DMSO-d6) δ 148.54, 134.35, 133.19, 132.24, 130.60, 129.03, 128.60, 126.74. Other characterization data are in accordance with that reported previously[37].

4.1.5.38. 2-(2-Phenylthiazol-4-yl)-1H-naphtho[2,3-d]imidazole-4,9-dione (**T38**)

Tan solid; yield 54%; m.p. >300□; ^{1}H NMR (400 MHz, DMSO-d6) δ 14.55 (s, 1H), 8.54 (s, 1H), 8.28 – 8.01 (m, 4H), 7.86 (s, 2H), 7.57 (s, 3H). ^{13}C NMR (101 MHz, DMSO-d6) δ 185.50, 168.37, 162.79, 148.39, 145.70, 134.33, 133.29, 132.96, 131.26, 129.70, 127.02, 126.76, 121.77. HR-ESI-MS: Calcd for $C_{20}H_{11}N_3O_2S$ $[M+H]^+$: 358.0645, found: 358.0643.

4.1.5.39. 2-(2-Methylthiazol-4-yl)-1H-naphtho[2,3-d]imidazole-4,9-dione (**T39**)

Tan solid; yield 58%; m.p. >300□; ^{1}H NMR (400 MHz, DMSO-d6) δ 14.46 (s, 1H), 8.35 (s, 1H), 8.09 (dd, J = 5.7, 3.3 Hz, 2H), 7.85 (dd, J = 5.7, 3.3 Hz, 2H), 2.79 (s, 3H). ^{13}C NMR (101 MHz, DMSO-d6) δ 178.95, 175.39, 167.42, 148.50, 144.57, 134.26, 133.26, 126.76, 121.55, 19.27. HR-ESI-MS: Calcd for $C_{15}H_9N_3O_2S$ $[M+H]^+$: 296.0488, found: 296.0490.

4.1.5.40. 2-(2-Bromothiazol-4-yl)-1H-naphtho[2,3-d]imidazole-4,9-dione (**T40**)

Tan solid; yield 66%; m.p. >300□; ^{1}H NMR (400 MHz, DMSO-d6) δ 14.65 (s, 1H), 8.55 (s, 1H), 8.11 (dd, J = 5.6, 3.3 Hz, 2H), 7.87 (dd, J = 5.6, 3.3 Hz, 2H). ^{13}C NMR (101 MHz, DMSO-d6) δ 147.22, 145.11, 138.06, 134.33, 133.26, 126.74, 126.17. HR-ESI-MS: Calcd for $C_{14}H_6BrN_3O_2S$ $[M+H]^+$: 359.9437, found: 359.9439.

4.1.5.41. 2-(2-Chlorothiazol-4-yl)-1H-naphtho[2,3-d]imidazole-4,9-dione (**T41**)

Tan solid; yield 68%; m.p. >300□; ^{1}H NMR (400 MHz, DMSO-d6) δ 14.66 (s, 1H), 8.52 (s, 1H), 8.12 (d, J = 5.1 Hz, 2H), 7.89 (d, J = 5.3 Hz, 2H). ^{13}C NMR (101 MHz, DMSO-d6) δ 199.89, 160.87, 152.52, 147.34, 143.50, 134.35, 133.28, 126.75, 124.67. HR-ESI-MS: Calcd for $C_{14}H_6ClN_3O_2S$ $[M+H]^+$: 315.9942, found: 315.9929.

4.1.5.42. 2-(Quinolin-4-yl)-1H-naphtho[2,3-d]imidazole-4,9-dione (**T42**)

Brown solid; yield 77%; m.p. >300□; ^{1}H NMR (400 MHz, DMSO-d6) δ 14.73 (s, 1H), 9.06 (d, J = 6.3 Hz, 1H), 8.15 – 8.07 (m, 3H), 8.04 (d, J = 4.6 Hz, 1H), 7.90 – 7.80 (m, 3H), 7.76 (t, J = 7.8 Hz, 1H). ^{13}C NMR (101 MHz, DMSO-d6) δ 150.53, 150.45, 148.88, 134.45, 133.40, 133.23, 130.36, 130.00, 128.22, 126.84, 124.85, 121.80. HR-ESI-MS: Calcd for $C_{20}H_{11}N_3O_2$ $[M+H]^+$: 326.0924, found: 326.0916.

4.1.5.43. 2-(2-Aminopyrimidin-5-yl)-1H-naphtho[2,3-d]imidazole-4,9-dione (**T43**)

Yellow solid; yield 70%; m.p. >300□; ^{1}H NMR (400 MHz, DMSO-d6) δ 14.12 (s, 1H), 8.96 (s, 2H), 8.05 (dd, J = 6.1, 3.0 Hz, 2H), 7.82 (dd, J = 6.1, 3.0 Hz, 2H), 7.28 (s, 2H). ^{13}C NMR (101 MHz, DMSO-d6) δ 164.15, 163.79, 162.27, 157.28, 150.19, 134.23, 133.12, 126.64, 112.44. HR-ESI-MS: Calcd for $C_{15}H_9N_5O_2$ $[M+H]^+$: 292.0829, found: 292.0813.

4.1.6. General procedure for the preparation of compounds T44-T47.

2-Amino-3-chloronaphthalene-1,4-dione (4.0mmol) was dissolved in a mixed solution of water and ethanol (3:1, 16 mL). Na_2S (6.25mmol) was added to the solution and the mixture was refluxed for 2 hours. Appropriate aromatic aldehyde was added and the solution was refluxed for another 2 hours. On completion of the reaction monitored by TLC, the precipitate

was filtered and purified by silica gel chromatography by DCM/MeOH system to afford the final product.

4.1.6.1. 2-(2-Aminopyrimidin-5-yl)-1H-naphtho[2,3-d]imidazole-4,9-dione (**T44**)

Brown solid; yield 72%; m.p. 304-306□; ^{1}H NMR (400 MHz, CF_3COOD) δ 8.71 (s, 2H), 8.49 (s, 2H), 8.10 (d, J=43.6, 2H), 7.66 (s, 2H). ^{13}C NMR (101 MHz, CF_3COOD) δ 181.49, 180.58, 168058, 156.84, 149.90, 146.95, 143.95, 137.44, 134.12, 133.27, 130.15, 129.52, 126.26. Other characterization data are in accordance with that reported previously[40].

4.1.6.2 2-(Pyridin-2-yl)naphtho[2,3-d]thiazole-4,9-dione (**T45**)

Brown solid; yield 62%; m.p. 295-297□; ^{1}H NMR (400 MHz, DMSO-d6) δ 8.77 (d, J = 4.8 Hz, 1H), 8.32 (d, J = 7.9 Hz, 1H), 8.26 – 8.02 (m, 3H), 7.94 (dd, J = 5.7, 3.4 Hz, 2H), 7.77 – 7.55 (m, 1H). Other characterization data are in accordance with that reported previously[40].

4.1.6.3. 2-(4-Nitrophenyl)naphtho[2,3-d]thiazole-4,9-dione (**T46**)

Pale yellow solid; yield 80% ; m.p. 278-280□; ^{1}H NMR (400 MHz, DMSO-d6) δ 8.85 (s, 1H), 8.59 (d, J = 7.8 Hz, 1H), 8.47 (d, J = 8.3 Hz, 1H), 8.22 (d, J = 7.0 Hz, 1H), 8.16 (d, J = 6.8 Hz, 1H), 8.05 – 7.83 (m, 3H). Other characterization data are in accordance with that reported previously[41].

4.1.6.4. 2-(Thiazol-4-yl)naphtho[2,3-d]thiazole-4,9-dione (**T47**)

Orange solid; yield 80%; m.p. 294-296□; ^{1}H NMR (400 MHz, DMSO-d6) δ 9.36 (s, 1H), 8.76 (s, 1H), 8.17 (d, J = 23.5 Hz, 2H), 7.93 (s, 2H). ^{13}C NMR (101 MHz, DMSO-d6) δ 178.76, 177.77, 168.08, 157.51, 155.40, 148.17, 142.02, 135.12, 134.74, 133.23, 133.05, 127.54, 126.84, 122.67. HR-ESI-MS: Calcd for $C_{14}H_6N_2O_2S_2$ $[M+H]^+$: 298.9943, found: 298.9936.

4.1.7. General procedure for the preparation of compounds T48-T50.

Compounds **T48**-**T50** were synthesized following the same route of compounds **T1**-**T44**

4.1.7.1. 2-(Pyridin-4-yl)-3H-imidazo[4,5-g]quinoline-4,9-dione (**T48**)

Tan solid; yield 70%; m.p. >300□; ^{1}H NMR (400 MHz, DMSO-d6) δ 14.87 (s, 1H), 9.01 (d, J = 4.6 Hz, 1H), 8.78 (d, J = 5.1 Hz, 2H), 8.48 (d, J = 7.9 Hz, 1H), 8.16 (d, J = 5.1 Hz, 2H), 7.85 (dd, J = 7.9, 4.8 Hz, 1H). Other characterization data are in accordance with that reported previously[42].

4.1.7.2. 2-(Thiazol-4-yl)-3H-imidazo[4,5-g]quinoline-4,9-dione (**T49**)

Brown solid; yield 62%; m.p. >300□; ^{1}H NMR (400 MHz, DMSO-d6) δ 14.64 (s, 1H), 9.34 (d, J = 1.9 Hz, 1H), 8.99 (d, J = 4.7 Hz, 1H), 8.58 (d, J = 2.0 Hz, 1H), 8.45 (d, J = 7.8 Hz, 1H), 7.83 (dd, J = 7.8, 4.7 Hz, 1H); ^{13}C NMR (101 MHz, DMSO-d6) δ 156.39, 153.83, 149.24, 148.68, 145.80, 134.74, 130.43, 127.95, 122.21. HR-ESI-MS: Calcd for $C_{13}H_6N_4O_2S$ $[M+H]^+$: 281.0139, found: 281.0132.

4.1.7.3. 2-(Pyridin-2-yl)-3H-imidazo[4,5-g]quinoline-4,9-dione (**T50**)

Yellow solid; yield 80%; m.p. >300□; ^{1}H NMR (400 MHz, DMSO-d6) δ 14.82 (s, 1H), 8.98 (dd, J = 4.6, 1.6 Hz, 1H), 8.74 (d, J = 4.8 Hz, 1H), 8.44 (dd, J = 7.9, 1.7 Hz, 1H), 8.27 (d, J = 7.9 Hz, 1H), 8.02 (td, J = 7.8, 1.7 Hz, 1H), 7.82 (dd, J = 7.9, 4.7 Hz, 1H), 7.56 (ddd, J = 7.5, 4.8, 1.2 Hz, 1H). ^{13}C NMR (101 MHz, DMSO) δ 153.86, 152.48, 150.00, 149.22, 147.57, 138.17, 134.76, 130.43, 127.96, 125.76, 122.65. HR-ESI-MS: Calcd for $C_{15}H_8N_4O_2$ $[M+H]^+$: 299.0539, found: 299.0568.

4.1.8. General procedure for the preparation of compounds T51-T54.

The mixture of **11a** and **11b** (4.0mmol) was dissolved in a mixed solution of water and ethanol (3:1, 16 mL). Na_2S (6.25mmol) was added to the solution and the mixture was refluxed for 2 hours. Appropriate aromatic aldehyde was added and the solution was refluxed for another 2 hours. On completion of the reaction monitored by TLC, the precipitate was filtered and purified by silica gel chromatography by DCM/MeOH system to afford the pure positional isomer.

4.1.8.1. 2-(Pyridin-4-yl)thiazolo[5,4-g]quinoline-4,9-dione (**T51**)

Brown solid; yield 54%; m.p. >300□; ^{1}H NMR (400 MHz, DMSO-d6) δ 9.09 (d, J = 4.7 Hz, 1H), 8.86 (d, J = 5.0 Hz, 2H), 8.60 (d, J = 7.9 Hz, 1H), 8.13 (d, J = 5.1 Hz, 2H), 7.94 (dd, J = 8.0, 4.8 Hz, 1H). ^{13}C NMR (101 MHz, DMSO-d6) δ 178.14, 175.79, 171.19, 155.51, 154.93, 151.59, 149.06, 142.55, 138.70, 134.91, 130.60, 128.37, 121.43. HR-ESI-MS: Calcd for $C_{15}H_7N_3O_2S$ $[M+H]^+$: 316.0151, found: 316.0148.

4.1.8.2. 2-(Pyridin-4-yl)thiazolo[5,4-g]quinoline-4,9-dione (**T52**)

Yellow solid; yield 21%; m.p. >300□; ^{1}H NMR (400 MHz, DMSO-d6) δ 9.13 (d, J = 4.7 Hz, 1H), 8.88 (d, J = 4.8 Hz, 2H), 8.56 (d, J = 7.8 Hz, 1H), 8.15 (d, J = 4.5 Hz, 2H), 7.95 (dd, J = 5.8, 3.5 Hz, 1H).

4.1.8.3. 2-(Thiazol-4-yl)thiazolo[4,5-g]quinoline-4,9-dione (**T53**)

Yellow solid; yield 50%。m.p. >300□; ^{1}H NMR (400 MHz, DMSO-d6) δ 9.37 (d, J = 2.0 Hz, 1H), 9.06 (dd, J = 4.5, 1.8 Hz, 1H), 8.78 (d, J = 2.0 Hz, 1H), 8.56 (dd, J = 7.9, 1.8 Hz, 1H), 7.92 (dd, J = 7.9, 4.6 Hz, 1H). ^{13}C NMR (101 MHz, DMSO-d6) δ 177.48, 177.01, 168.17, 157.60, 154.84, 154.32, 149.12, 148.07, 142.75, 135.48, 130.43, 128.60, 122.87. HR-ESI-MS: Calcd for $C_{13}H_5N_3O_2S_2$ $[M+H]^+$: 299.9896, found: 299.9909.

4.1.8.4. 2-(Thiazol-4-yl)thiazolo[5,4-g]quinoline-4,9-dione (**T54**)

Yellow solid; yield 23%; m.p. >300□; ^{1}H NMR (400 MHz, DMSO-d6) δ 9.37 (d, J = 1.8 Hz, 1H), 9.08 (dd, J = 4.5, 1.8 Hz, 1H), 8.79 (d, J = 1.9 Hz, 1H), 8.51 (d, J = 7.9 Hz, 1H), 7.91 (dd, J = 7.9, 4.6 Hz, 1H). ^{13}C NMR (101 MHz, DMSO-d6) δ 178.26, 175.99, 168.15, 157.62, 155.77, 154.73, 148.99, 148.10, 141.20, 134.77, 130.58, 128.29, 122.90. HR-ESI-MS: Calcd for $C_{13}H_5N_3O_2S_2$ $[M+H]^+$: 299.9896, found: 299.9888.

4.1.9. General procedure for the preparation of compounds **T55**-**T60**.

To a suspension of the 1H-naphtho[2,3-d]imidazole-4,9-dione derivatives (1mmol) in

acetonitrile (10mL) was added caesium carbonate (1.5mmol) and the corresponding alkyl bromide (1.05mmol). The reaction mixture was stirred at room temperature for 1-3 hours and after this time it was concentrated in vacuo. The residue was suspended in a mixture of CH_2Cl_2 and sat. $NaHCO_3$. The aqueous layer was extracted with CH_2Cl_2 (2x30mL). The combined organic layers were dried over Na_2SO_4, filtered and the solvent was removed under reduced pressure. The crude product was purified by flash chromatography

4.1.9.1. 1-(2-Methylbenzyl)-2-(pyridin-4-yl)-1H-naphtho[2,3-d]imidazole-4,9-dione (**T55**)

Yellow solid; yield 77%; m.p. >300□; ^{1}H NMR (400 MHz, DMSO-d6) δ 8.73 (d, J = 6.1 Hz, 2H), 8.17 (dd, J = 7.5, 1.6 Hz, 1H), 8.03 (dd, J = 7.1, 1.8 Hz, 1H), 7.92 – 7.84 (m, 2H), 7.62 – 7.58 (m, 2H), 7.27 (d, J = 7.5 Hz, 1H), 7.19 (t, J = 7.5 Hz, 1H), 7.07 (t, J = 7.4 Hz, 1H), 6.60 (d, J = 7.7 Hz, 1H), 5.79 (s, 2H), 2.34 (s, 3H). ^{13}C NMR (101 MHz, DMSO-d6) δ 178.84, 176.25, 152.18, 150.86, 143.67, 135.98, 134.99, 134.81, 134.75, 134.52, 133.95, 133.25, 133.03, 130.78, 127.86, 126.98, 126.75, 124.38, 123.14, 109.99, 48.21, 19.13. HR-ESI-MS: Calcd for $C_{24}H_{17}N_3O_2$ $[M+H]^+$: 402.1213, found: 402.1208.

4.1.9.2. 1-(3-Chlorobenzyl)-2-(pyridin-4-yl)-1H-naphtho[2,3-d]imidazole-4,9-dione (**T56**)

Brown solid; yield 56%; m.p. 178-180□; ^{1}H NMR (400 MHz, DMSO-d6) δ 8.74 (d, J = 5.0 Hz, 2H), 8.14 (d, J = 6.7 Hz, 1H), 8.05 (d, J = 7.0 Hz, 1H), 7.93 – 7.81 (m, 2H), 7.62 (d, J = 4.4 Hz, 2H), 7.38 – 7.30 (m, 2H), 7.27 (s, 1H), 7.05 (d, J = 5.2 Hz, 1H), 5.87 (s, 2H). ^{13}C NMR (101 MHz, DMSO-d6) δ 178.85, 176.48, 151.89, 150.86, 143.51, 138.91, 135.99, 134.76, 134.47, 133.98, 133.89, 133.33, 132.99, 131.18, 128.19, 126.93, 126.76, 126.55, 125.10, 123.37, 49.16.

HR-ESI-MS: Calcd for $C_{23}H_{14}ClN_3O_2$ $[M+H]^+$: 422.0667, found: 422.0664.

4.1.9.3. 1-(3-Chlorobenzyl)-1H-naphtho[2,3-d]imidazole-4,9-dione (**T57**)

Brown solid; yield 82%; m.p. 185-187□; ^{1}H NMR (400 MHz, DMSO-d6) δ 8.52 (s, 1H), 8.12 – 8.00 (m, 2H), 7.91 – 7.77 (m, 2H), 7.46 (s, 1H), 7.41 – 7.34 (m, 2H), 7.34 – 7.23 (m, 1H), 5.68 (s, 2H). ^{13}C NMR (101 MHz, $CDCl_3$) δ 178.74, 176.66, 144.34, 144.10, 136.87, 135.04,

134.12, 133.60, 132.99, 132.89, 131.58, 130.47, 128.96, 127.86, 127.23, 126.62, 125.89, 49.77. HR-ESI-MS: Calcd for $C_{18}H_{11}ClN_2O_2$ $[M+H]^+$: 323.0587, found: 323.0587.

4.1.9.4. Methyl 3-((4,9-dioxo-4,9-dihydro-1H-naphtho[2,3-d]imidazol-1-yl)methyl)benzoate (**T58**)

Brown solid; yield 78%; m.p. 226-228□; ^{1}H NMR (400 MHz, DMSO-d6) δ 8.57 (s, 1H), 8.11-8.06 (m, 1H), 8.05-8.01 (m, 1H), 7.98 (s, 1H), 7.89 (d, J = 7.7 Hz, 1H), 7.86-7.81 (m, 2H), 7.62 (d, J = 7.8 Hz, 1H), 7.52 (t, J = 7.7 Hz, 1H), 5.74 (s, 2H), 3.84 (s, 3H). ^{13}C NMR (101 MHz, DMSO-d6) δ 178.81, 176.34, 166.35, 146.10, 144.08, 137.58, 134.68, 134.31, 133.14, 133.00, 132.79, 132.12, 130.46, 129.77, 129.19, 128.62, 126.94, 126.62, 52.74, 49.44. HR-ESI-MS: Calcd for $C_{21}H_{16}N_2O_4$ $[M+H]^+$: 317.1068, found: 317.1060.

4.1.9.5. 1-(2-Methylbenzyl)-1H-naphtho[2,3-d]imidazole-4,9-dione (**T59**)

Yellow solid; yield 82%; m.p. 214-216□; ^{1}H NMR (400 MHz, DMSO-d_6) δ 8.33 (s, 1H), 8.13 – 8.08 (m, 1H), 8.00 (dd, *J* = 7.0, 1.9 Hz, 1H), 7.90 – 7.78 (m, 2H), 7.26 (d, *J* = 7.5 Hz, 1H), 7.20 (t, *J* = 7.4 Hz, 1H), 7.11 (t, *J* = 7.5 Hz, 1H), 6.71 (d, *J* = 7.6 Hz, 1H), 5.68 (s, 2H), 2.39 (s, 3H). ^{13}C NMR (101 MHz, DMSO-d6) δ 178.85, 176.30, 146.26, 144.01, 135.66, 135.02, 134.65, 134.30, 133.19, 133.03, 132.51, 130.69, 128.09, 126.94, 126.80, 126.57, 126.13, 47.95, 19.18. HR-ESI-MS: Calcd for $C_{19}H_{14}N_2O_2$ $[M+H]^+$: 303.1134, found: 303.1137.

4.1.9.6. 3-((4,9-Dioxo-4,9-dihydro-1H-naphtho[2,3-d]imidazol-1-yl)methyl)benzoic acid (**T60**)

Yellow solid; yield 80%; m.p. >200□; ^{1}H NMR (400 MHz, DMSO-d_6) δ 12.20 (s, 1H), 8.56 (s, 1H), 8.07 (dd, *J* = 20.1, 7.0 Hz, 2H), 7.94 (s, 1H), 7.91 – 7.80 (m, 3H), 7.60 (d, *J* = 7.7 Hz, 1H), 7.50 (t, *J* = 7.7 Hz, 1H), 5.74 (s, 2H). ^{13}C NMR (101 MHz, DMSO-d6) δ 178.80, 176.36, 174.99, 173.54, 167.40, 146.10, 144.09, 137.35, 134.67, 134.30, 133.02, 132.37, 131.67, 129.55, 128.71, 126.95, 126.63, 57.50.

4.2. Biological evaluations

4.2.1. IDO-1 Inhibition Assay

IDO1 catalyzes the oxidative cleavage of the pyrrole ring of the indole nucleus of tryptophan to yield N-formyl-kynurenine. The assays were performed at room temperature as described in the literature using 20 nM IDO and 2 mM D-Trp in the presence of 20 mM ascorbate, 3.5 μM methylene blue and 0.2 mg/mL catalase in 50 mM potassium phosphate buffer (pH 6.5). The initial reaction rates were recorded by continuously following the absorbance increase at 321 nm due to the formation of N-formyl-kynurenine. The IC_{50} values were calculated using nonlinear regression with normalized dose−response fit using Prism GraphPad software.

4.2.2. TDO Inhibition Assay

The assay was performed by UV absorption using recombinant TDO and L-Tryptophan as the substrate. The UV absorption signal at 321 nm is correlated with the amount of N-formylkynurenine reaction product of TDO. All of the reactions were conducted at room temperature. The 100 μL reaction mixture in TDO Assay Buffer contains 50 nM TDO, the indicated amount of the inhibitor, 200 μM tryptophan, and the coupled reaction components. The reaction mixture incubated for 75 min prior to reading the UV absorption signal. For the negative control (blank), 5 μL of the assay buffer was added instead of the TDO. The initial reaction rates were recorded by continuously following the absorbance increase at 321 nm due to the formation of N-formlylkynurenine. The IC_{50} values were calculated using nonlinear regression with normalized dose−response fit using Prism GraphPad software.

4.2.3. Kynurenine Generation Suppression Assay

SD rats (250-300g) were chosen to determine the effect of IDO inhibition on plasma kynurenine. A single intragastric 50 mg/kg dose of corresponding compounds was administered to 3 rats. Blood was harvested from the rat eye socket at various time points after dosing over 8 h (0h, 1h, 2h, 3h, 4h, 6h, 8h). The blood sample was centrifuged for 10

mins at 3000RPM and the supernatant was got. Kynurenine concentrations were measured by enzyme-linked immunosorbent assay kit.

4.2.4. MTT assay of cell viability

Human cells [human cervical carcinoma cell (HeLa), breast carcinoma cell (MCF-7), and embryonic kidney cells (HEK293T)] were seeded in each well of 96-well culture plate (3-4×10^3 per well). After overnight incubation, solution of compounds in DMSO (10 mM) was added to the cells. Cells treated with DMSO 1% were used as negative control. After further incubation for 48 h, MTT solution (5 mg/mL in PBS) was added to each well. After incubation for 4 h at 37 °C, MTT solution was removed and 150 μL of DMSO was added to dissolve the crystals formed. Then, absorbance at 570 nm was read using a microplate reader. The IC_{50} values were calculated using Prism 5.0.

4.2.5. LDH cytotoxicity assay

Human cells [human cervical carcinoma cell (HeLa) and embryonic kidney cells (HEK293T)] were seeded in each well of 96-well culture plate (3-4×10^3 per well). After target compounds treatment for 24 h in DMEM, the supernatant was got through centrifugation for 5 minutes. The LDH release activity was determined using an LDH cytotoxicity assay kit (Beyotime, Haimen, Jiangsu, China) according to the manufacturer's instructions. The absorbance was measured at 490 nm by a microplate reader within 1 h. The cytotoxicity was expressed using the formula: Cytotoxicity (%) = (OD_{Sample}-$OD_{Control}$) / ($OD_{Maximum\ release}$- $OD_{Control}$) x 100.

Acknowledgment

We gratefully acknowledge the National Natural Science Foundation of China (NSFC No. 81573272) and Beijing Natural Science Foundation (No. 7162109) for generous financial supports.

References

[1] H. Li, K.B. Chiappinelli, A.A. Guzzetta, H. Easwaran, R.W.C. Yen, R. Vatapalli, M.J. Topper, J. Luo, R.M.

Connolly, N.S. Azad, Immune regulation by low doses of the DNA methyltransferase inhibitor 5-azacitidine in common human epithelial cancers, Oncotarget, 5 (2014) 587.

[2] D.S. Vinay, E.P. Ryan, G. Pawelec, W.H. Talib, J. Stagg, E. Elkord, T. Lichtor, W.K. Decker, R.L. Whelan, H.M.C.S. Kumara, Immune evasion in cancer: Mechanistic basis and therapeutic strategies, Semin. Cancer Biol., 35 (2015) S185-S198.

[3] D.H. Munn, A.L. Mellor, IDO in the tumor microenvironment: iInflammation, counter-regulation, and tolerance, Trends Immunol., 37 (2016) 193.

[4] I.T. Zeeberg, A.M. Hald, S.I. Marie, The targeting of IDO-mediated immune escape in cancer, Basic Clin. Pharmacol. Toxicol., 116 (2014) 19–24.

[5] G.C. Prendergast, Immune escape as a fundamental trait of cancer: focus on IDO, Oncogene, 27 (2008) 3889-3900.

[6] J.B. Katz, A.J. Muller, G.C. Prendergast, Indoleamine 2,3-dioxygenase in T-cell tolerance and tumoral immune escape, Immunol. Rev., 222 (2008) 206-221.

[7] M. Zamanakou, A.E. Germenis, V. Karanikas, Tumor immune escape mediated by indoleamine 2,3-dioxygenase, Immunol. Lett., 111 (2007) 69-75.

[8] L. Capece, A. Lewis-Ballester, D. Batabyal, R.N. Di, S.R. Yeh, D.A. Estrin, M.A. Marti, The first step of the dioxygenation reaction carried out by tryptophan dioxygenase and indoleamine 2,3-dioxygenase as revealed by quantum mechanical/molecular mechanical studies, J. Biol. Inorg. Chem., 15 (2010) 811-823.

[9] J.T. Pearson, S. Siu, D.P. Meininger, L.C. Wienkers, A.R. Dan, In vitro modulation of cytochrome P450 reductase supported indoleamine 2,3-dioxygenase activity by allosteric effectors cytochrome b5 and methylene blue, Biochemistry, 49 (2010) 2647-2656.

[10] L. Vecsei, L. Szalardy, F. Fulop, J. Toldi, Kynurenines in the CNS: recent advances and new questions, Nat. Rev. Drug Disc., 12 (2013) 64-82.

[11] M. Platten, W. Wick, V.D.E. Bj, Tryptophan catabolism in cancer: beyond IDO and tryptophan depletion, Cancer Res., 72 (2012) 5435.

[12] I. Théate, B.N. Van, L. Pilotte, P. Moulin, P. Larrieu, J.C. Renauld, C. Hervé, I. Gutierrezroelens, E. Marbaix, C. Sempoux, Extensive profiling of the expression of the indoleamine 2,3-dioxygenase 1 protein in normal and tumoral human tissues, Cancer Immunol Res, 3 (2014).

[13] M.T. Pallotta, C. Orabona, C. Volpi, C. Vacca, M.L.L. Belladonna, R. Bianchi, G. Servillo, C. Brunacci, M.

Calvitti, S. Bicciato, Pallotta, M.T. et al. Indoleamin 2,3-dioxygenase is a signaling protein in long-term tolerance by dendritic cells. Nat. Immunol 12, 870-878, Nat. Immunol., 12 (2011) 870-878.

[14] M.W. Taylor, G.S. Feng, Relationship between interferon-gamma, indoleamine 2,3-dioxygenase, and tryptophan catabolism, Faseb Journal Official Publication of the Federation of American Societies for Experimental Biology, 5 (1991) 2516.

[15] R. Metz, S. Rust, J.B. DuHadaway, M.R. Mautino, D.H. Munn, N.N. Vahanian, C.J. Link, G.C. Prendergast, IDO inhibits a tryptophan sufficiency signal that stimulates mTOR: A novel IDO effector pathway targeted by D-1-methyl-tryptophan, Oncoimmunology, 1 (2012) 1460.

[16] D.H. Munn, M.D. Sharma, B. Baban, H.P. Harding, Y. Zhang, D. Ron, A.L. Mellor, GCN2 kinase in T cells mediates proliferative arrest and anergy induction in response to indoleamine 2,3-dioxygenase, Immunity, 22 (2005) 633-642.

[17] J.D. Mezrich, J.H. Fechner, X. Zhang, B.P. Johnson, W.J. Burlingham, C.A. Bradfield, An Interaction between Kynurenine and the Aryl Hydrocarbon Receptor Can Generate Regulatory T Cells, J. Immunol., 185 (2010) 3190.

[18] T. Jinushi, Y. Shibayama, I. Kinoshita, S. Oizumi, M. Jinushi, T. Aota, T. Takahashi, S. Horita, H. Dosaka□ Akita, K. Iseki, Low expression levels of microRNA□124□5p correlated with poor prognosis in colorectal cancer via targeting of SMC4, Cancer Medicine, 3 (2014) 1544-1552.

[19] K.A. Shirey, J.Y. Jung, G.S. Maeder, J.M. Carlin, Upregulation of IFN-γ Receptor Expression by Proinflammatory Cytokines Influences IDO Activation in Epithelial Cells, Journal of Interferon & Cytokine Research the Official Journal of the International Society for Interferon & Cytokine Research, 26 (2006) 53-62.

[20] H. Song, H. Park, Y.S. Kim, K.D. Kim, H.K. Lee, D.H. Cho, J.W. Yang, D.Y. Hur, L-kynurenine-induced apoptosis in human NK cells is mediated by reactive oxygen species, Int. Immunopharmacol., 11 (2011) 932-938.

[21] H. Sugimoto, S. Oda, T. Otsuki, T. Hino, T. Yoshida, Y. Shiro, Crystal structure of human indoleamine 2,3-dioxygenase: catalytic mechanism of O2 incorporation by a heme-containing dioxygenase, Proc. Natl. Acad. Sci. U. S. A., 103 (2006) 2611-2616.

[22] S. Kumar, W.P. Malachowski, J.B. Duhadaway, J.M. Lalonde, P.J. Carroll, D. Jaller, R. Metz, G.C. Prendergast, A.J. Muller, Indoleamine 2,3-dioxygenase is the anticancer target for a novel series of potent

naphthoquinone-based inhibitors, J. Med. Chem., 51 (2008) 1706-1718.

[23] B. Chesneau, M. Hardouin-Lerouge, P. Hudhomme, A fused donor-acceptor system based on an extended tetrathiafulvalene and a ruthenium complex of dipyridoquinoxaline, Org. Lett., 12 (2010) 4868-4871.

[24] E.W. Yue, B. Douty, B. Wayland, M. Bower, X. Liu, L. Leffet, Q. Wang, K.J. Bowman, M.J. Hansbury, C. Liu, Discovery of potent competitive inhibitors of indoleamine 2,3-dioxygenase with in vivo pharmacodynamic activity and efficacy in a mouse melanoma model, J. Med. Chem., 52 (2009) 7364.

[25] A. Curti, S. Trabanelli, V. Salvestrini, M. Baccarani, R.M. Lemoli, The role of indoleamine 2,3-dioxygenase in the induction of immune tolerance: focus on hematology, Blood, 113 (2009) 2394-2401.

[26] R. Schwarcz, J.P. Bruno, P.J. Muchowski, H.Q. Wu, Kynurenines in the mammalian brain: when physiology meets pathology, Nat Rev Neurosci, 13 (2012) 465-477.

[27] S.J. Thackray, C.G. Mowat, S.K. Chapman, Exploring the mechanism of tryptophan 2,3-dioxygenase, Biochem. Soc. Trans., 36 (2008) 1120.

[28] L. Pilotte, P. Larrieu, V. Stroobant, D. Colau, E. Dolušić, R. Frédérick, E.D. Plaen, C. Uyttenhove, J. Wouters, B. Masereel, Reversal of tumoral immune resistance by inhibition of tryptophan 2,3-dioxygenase, Proc. Natl. Acad. Sci. U. S. A., 109 (2012) 2497.

[29] C.A. Opitz, U.M. Litzenburger, F. Sahm, M. Ott, I. Tritschler, S. Trump, T. Schumacher, L. Jestaedt, D. Schrenk, M. Weller, An endogenous tumour-promoting ligand of the human aryl hydrocarbon receptor, Nature, 478 (2011) 197.

[30] T. Jean-Luc, F. Anita, E. Eric, Method for industrial production of naphtho-[2,3-d]-thiazole compounds, WO9837076 , 1998.

[31] R. DíAz, O. Reyes, A. Francois, A.M.A. Leiva, B. Loeb, Synthesis of a new polypyridinic highly conjugated ligand with electron-acceptor properties, Tetrahedron Lett., 42 (2001) 6463-6467.

[32] B.J. Mulchin, C.G. Newton, J.W. Baty, C.H. Grasso, W.J. Martin, M.C. Walton, E.M. Dangerfield, C.H. Plunkett, M.V. Berridge, J.L. Harper, The anti-cancer, anti-inflammatory and tuberculostatic activities of a series of 6,7-substituted-5,8-quinolinequinones, Biorg. Med. Chem., 18 (2010) 3238-3251.

[33] E.Y. Yoon, Y.C. Han, K.J. Shin, K.H. Yoo, D.Y. Chi, J.K. Dong, The regioselectivity in the reaction of 6,7-dihaloquinoline-5,8-diones with amine nucleophiles in various solvents, Tetrahedron Lett., 31 (2000) 7475-7480.

[34] S.H. Ho, M.Y. Sim, W.L. Yee, T. Yang, S.P. Yuen, M.L. Go, Antiproliferative, DNA intercalation and redox

cycling activities of dioxonaphtho[2,3-d]imidazolium analogs of YM155: a structure-activity relationship study, Eur. J. Med. Chem., 104 (2015) 42-56.

[35] V.K. Tandon, M.K. Verma, H.K. Maurya, S. Kumar, Micelles catalyzed one pot regio- and chemoselective synthesis of benzo[a]phenazines and naphtho[2,3-d]imidazoles 'in H_2O', Tetrahedron Lett., 55 (2014) 6331-6334.

[36] O. Boutherin-Falson, S. Desquand-Billiald, A. Favrou, M. Finet, O. Tembo, J.L. Torregrosa, S. Yannic-Arnoult, F. Domagala-Le Marquer, Use of tricyclic 1,4-dihydro-1,4-dioxo-1*H*-naphthalene derivatives, resulting novel compounds abd therapeutical use thereof, EP0876356, 1997.

[37] R. Manivannan, A. Satheshkumar, K.P. Elango, Tuning of the H-bonding ability of imidazole N–H towards the colorimetric sensing of fluoride and cyanide ions as their sodium salts in water, New J. Chem., 37 (2013) 3152-3160.

[38] J. Lee, H. Kim, M.J. Park, Long-life, high-rate lithium-organic batteries based on naphthoquinone derivatives, Chem. Mater., 28 (2016), 2408-2416.

[39] A.A. Aly, A.A. Hassan, A.B. Brown, K.M. El-Shaieb, T.M.I. Bedair, Facile synthesis of new imidazoles from direct reaction of 2,3-diamino-1,4-naphthoquinone with aldehydes, J. Heterocycl. Chem., 48 (2011) 787-791.

[40] A.R. Katritzky, W.Q. Fan, Some novel quinone-type dyes containing naphthoquinone and related fused ring systems, J. Heterocycl. Chem., 25 (2010) 901-906.

[41] J. Gao, Y. Zheng, Study of third order nonlinear optical properties of dioxonaphthothiazole compounds, Chin. J. Lasers, DOI (1998) 163-167.

[42] S. Carl-Wolfgang, P. Siegfried, D. Gerhard, Quinone derivatives and processes for producing the same, US3084165, 1963.

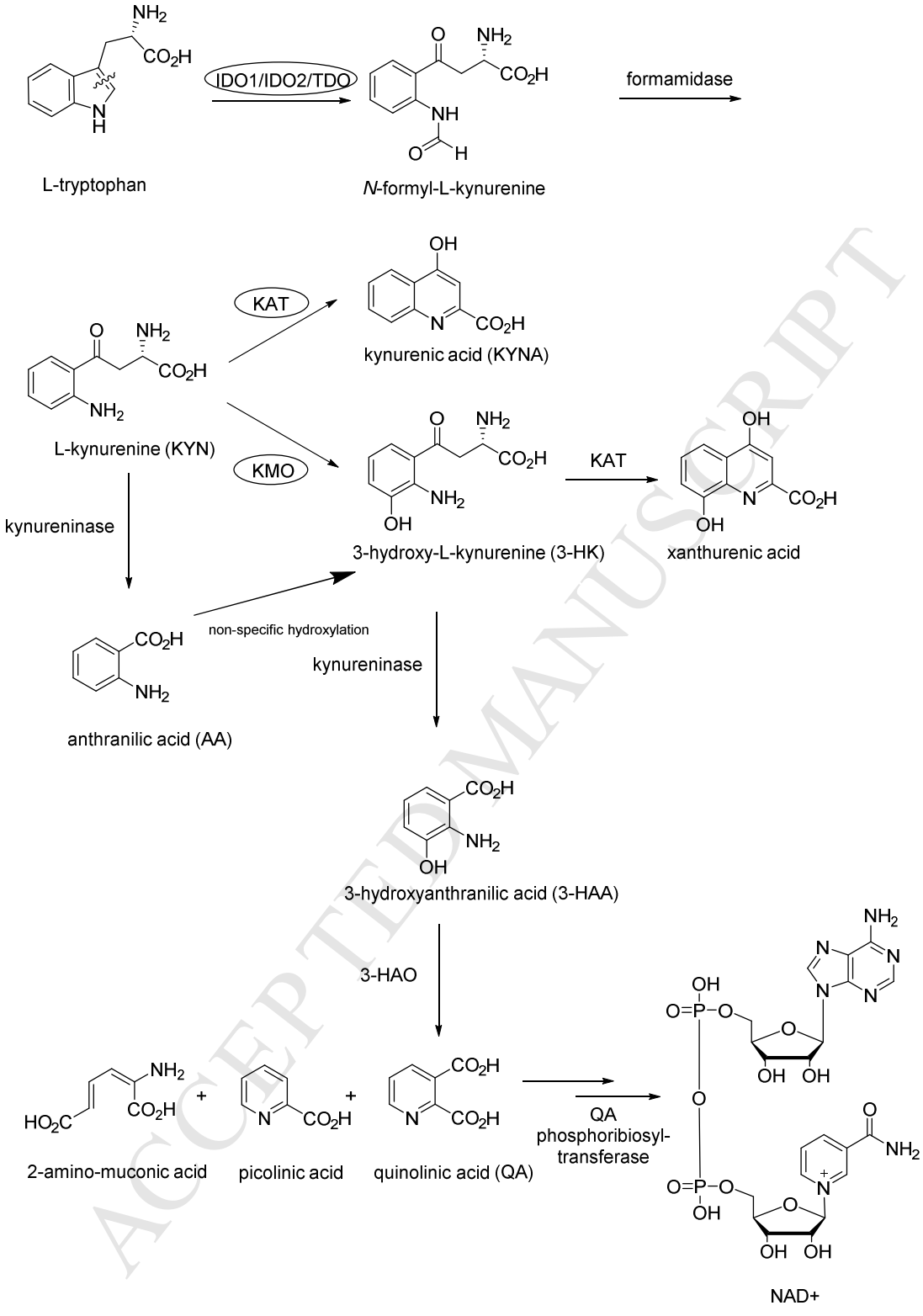

Figure 1. The kynurenine pathway of tryptophan catabolism in mammals

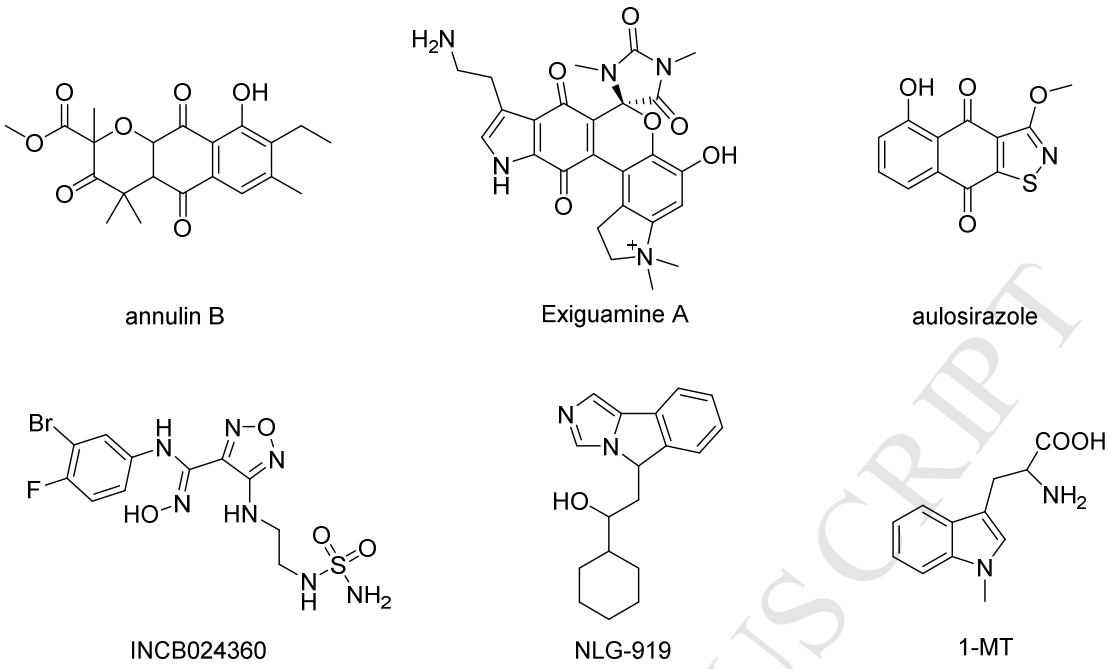

Figure 2. Structures of representative IDO1 inhibitors

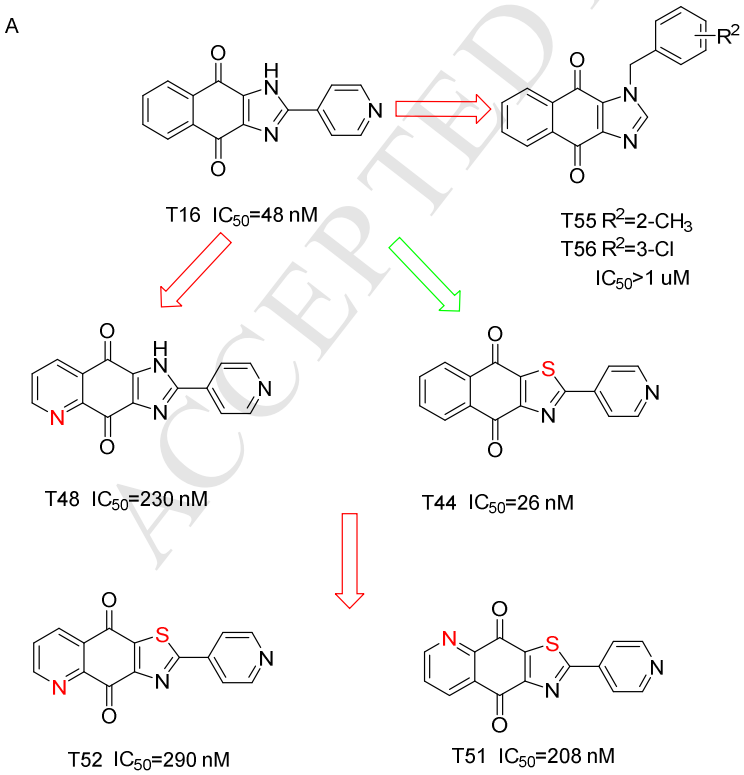

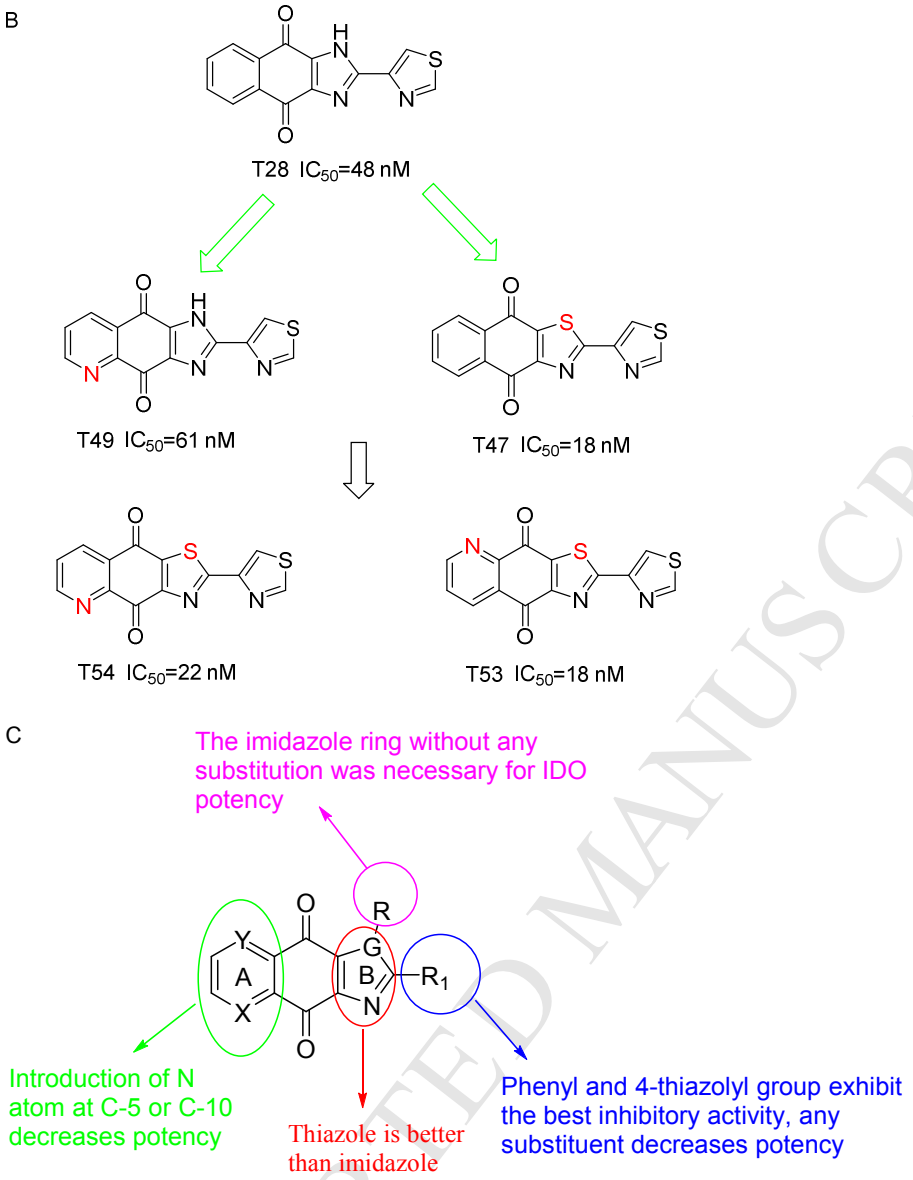

Figure 3. (A)：Structure and inhibitor activity of **T16** derivatives. (B)：Structure and inhibitor activity of **T28** derivatives. (C): Preliminary SAR of synthesized naphthoquinone derivatives.

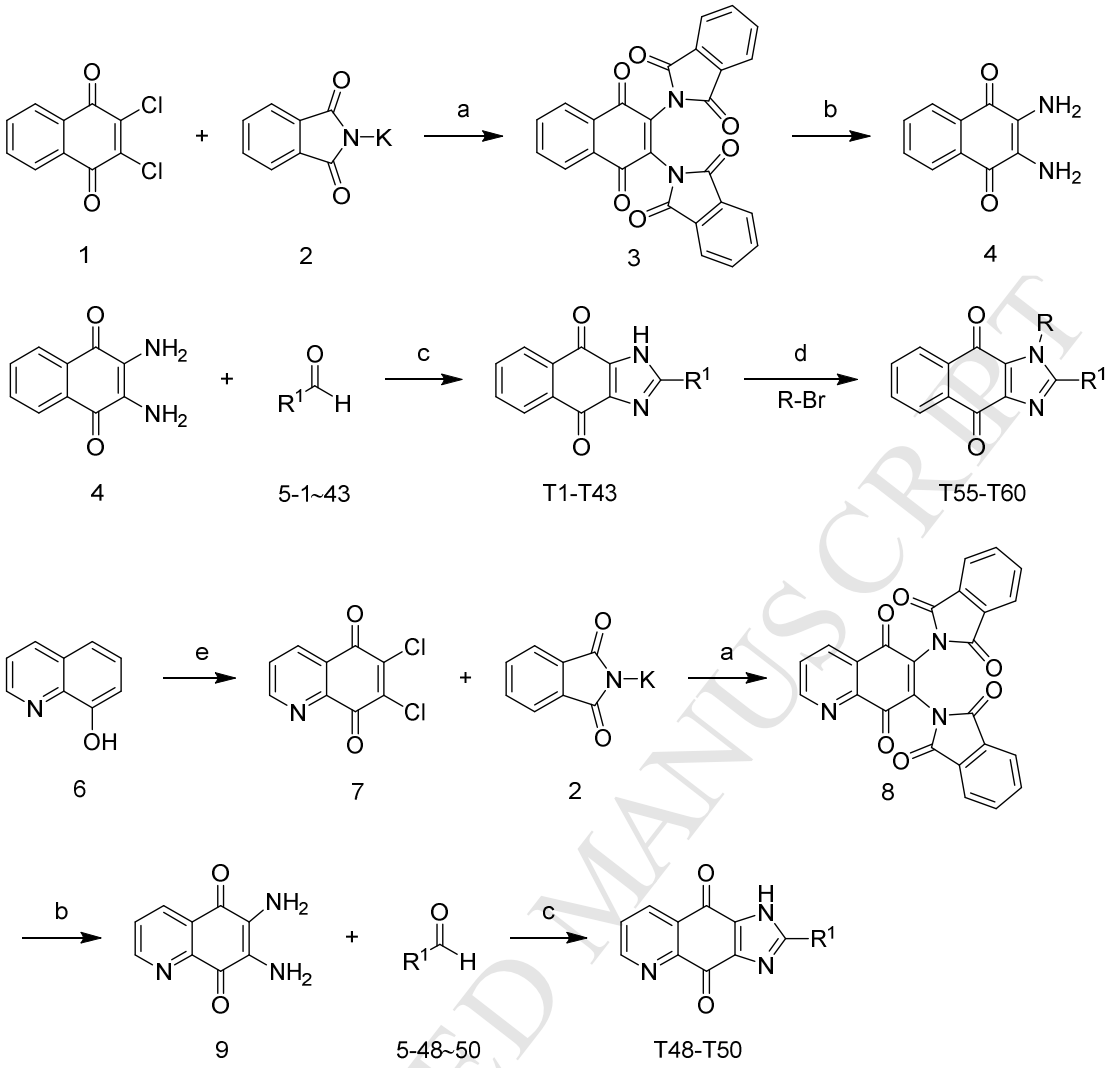

Scheme 1.

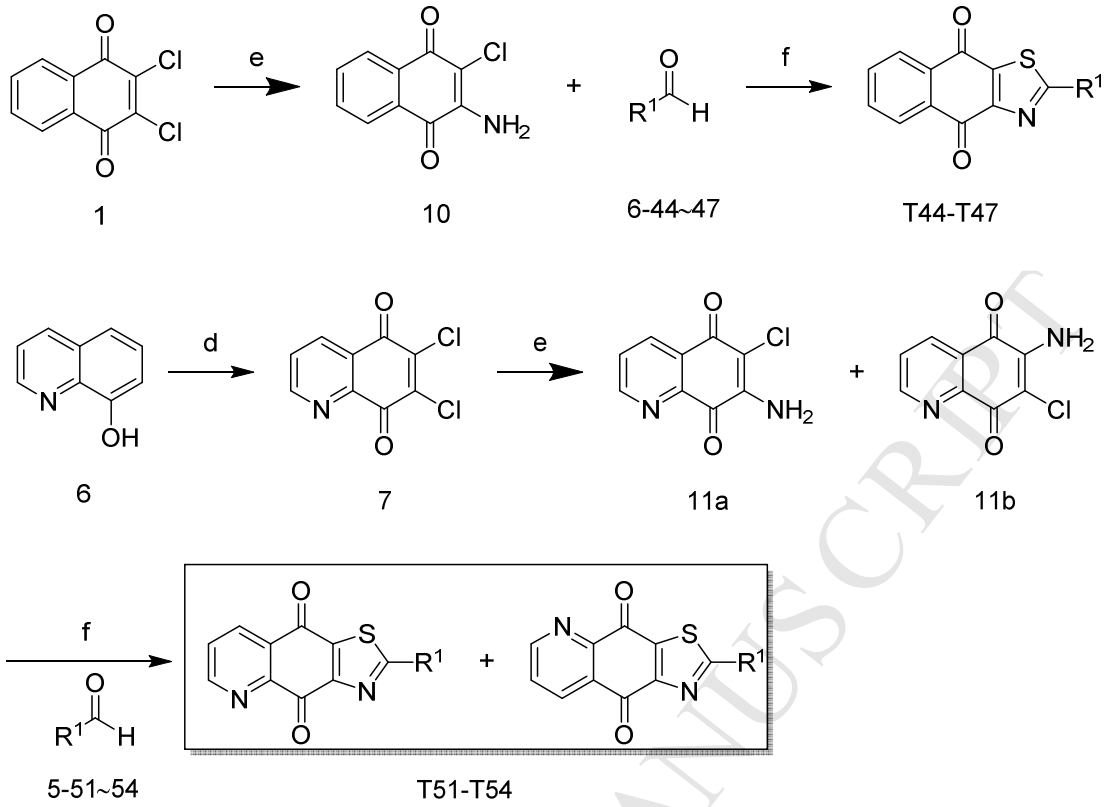

Scheme 2.

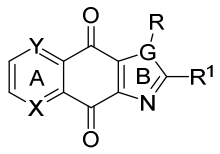

Table 1. Structures of naphthoquinone derivatives

No.	X	Y	G	R^1	R
T1	C	C	N	2-chlorophenyl	H
T2	C	C	N	3-chlorophenyl	H
T3	C	C	N	4-chlorophenyl	H
T4	C	C	N	2-fluorophenyl	H
T5	C	C	N	4-fluorophenyl	H
T6	C	C	N	2-bromophenyl	H
T7	C	C	N	2-methoxyphenyl	H
T8	C	C	N	3-methoxyphenyl	H
T9	C	C	N	4-methoxyphenyl	H
T10	C	C	N	3-cyanophenyl	H
T11	C	C	N	4-cyanophenyl	H
T12	C	C	N	4-(methoxycarbonyl)phenyl	H
T13	C	C	N	4-carboxyphenyl	H
T14	C	C	N	4-nitrophenyl	H
T15	C	C	N	3-nitrophenyl	H
T16	C	C	N	4-pyridyl	H
T17	C	C	N	3-pyridyl	H
T18	C	C	N	2-pyridyl	H
T19	C	C	N	3-fluoropyridin-4-yl	H
T20	C	C	N	2-methoxypyridin-4-yl	H
T21	C	C	N	2-hydroxypyridin-4-yl	H
T22	C	C	N	3-chloropyridin-4-yl	H
T23	C	C	N	2-chloropyridin-4-yl	H
T24	C	C	N	3-fluoro-1-oxidopyridin-4-yl	H
T25	C	C	N	H	H
T26	C	C	N	methyl	H
T27	C	C	N	5-thiazolyl	H
T28	C	C	N	4-thiazolyl	H
T29	C	C	N	4-imidazolyl	H
T30	C	C	N	4-pyrazolyl	H
T31	C	C	N	2-thiazolyl	H
T32	C	C	N	3-pyrryl	H
T33	C	C	N	2-imidazolyl	H
T34	C	C	N	3-pyrazolyl	H
T35	C	C	N	2-pyrryl	H
T36	C	C	N	2-indolyl	H
T37	C	C	N	2-thienyl	H

T38	C	C	N	2-phenylthiazol-4-yl	H
T39	C	C	N	2-methylthiazol-4-yl	H
T40	C	C	N	2-bromothiazol-4-yl	H
T41	C	C	N	2-chlorothiazol-4-yl	H
T42	C	C	N	4-quinolyl	H
T43	C	C	N	2-aminopyrimidin-5-yl	H
T44	C	C	S	4-pyridyl	H
T45	C	C	S	2-pyridyl	H
T46	C	C	S	4-nitrophenyl	H
T47	C	C	S	4-thiazolyl	H
T48	N	C	N	4-pyridyl	H
T49	N	C	N	4-thiazolyl	H
T50	N	C	N	2-pyridyl	H
T51	N	C	S	4-pyridyl	H
T52	C	N	S	4-pyridyl	H
T53	N	C	S	4-thiazolyl	H
T54	C	N	S	4-thiazolyl	H
T55	C	C	N	4-thiazolyl	2-methylbenzyl
T56	C	C	N	4-thiazolyl	3-chlorobenzyl
T57	C	C	N	H	3-chlorobenzyl
T58	C	C	N	H	3-(methoxycarbonyl)benzyl
T59	C	C	N	H	2-methylbenzyl
T60	C	C	N	H	3-carboxybenzyl

Table 2. Inhibitory rate (at 1μM) and IC_{50} (nM) values of the compounds **T1-18**, **T27-37** and **T42-43** derivatives against IDO1

No.	% inhibition	IDO IC_{50}(nM)	SD
T1	34	-	-
T2	59	577.2	37.6
T3	20.5	-	-
T4	38	-	-
T5	16.5	-	-
T6	33.5	-	-
T7	38	-	-
T8	30.5	-	-
T9	27.5	-	-
T10	34.5	-	-
T11	66.5	597.8	44.0
T12	38	11000	500
T13	28	-	-
T14	62	590	11.3
T15	46	-	-
T16	79	48	5.6
T17	58	-	-
T18	56	-	-
T27	38	2700	0.0
T28	74.5	119.6	8.3
T29	34	7800	0.0
T30	53.5	-	-
T31	37.5	-	-
T32	67.5	684	251
T33	74.5	134	35.4
T34	46	-	-
T35	44.5	-	-
T36	17.5	-	-
T37	57	-	-
T42	28	9500	300
T43	53.5	1500	100
INCB24360	93	64.6	0.1

-: Not detected; SD: Standard deviation for at least two runs.

Table 3. Inhibitory rate (at 1μM) and IC_{50} (nM) values of the compounds **T19-24**, **T38-41** derivatives against IDO1

No.	% inhibition	IDO IC_{50}(nM)	SD
T19	42	-	-
T20	51.5	1100	100
T21	37	-	-
T22	45	2200	0.0
T23	45	151.8	10.1
T24	30.5	-	-
T38	12	-	-
T39	50	-	-
T40	37	-	-
T41	15	-	-
INCB024360	93	64.6	0.1

-: Not detected; SD: Standard deviation for at least two runs.

Table 4. Inhibitory rates (at 1μM) and IC_{50} (nM) values of the compounds **T44-60** against IDO1

No.	% inhibition	IDO IC_{50}(nM)	SD
T44	88	26.2	1.2
T45	74	29	5.7
T46	-	-	-
T47	76	18	11.3
T48	65.5	233.7	14.3
T49	76	61	7.8
T50	71.5	338	79.2
T51	73	207.9	3.6
T52	70.5	289.5	23.2
T53	73.5	18	4.9
T54	69.5	22	8.5
T55	9	50300	6600
T56	26	3300	200
T57	16	>100000	-
T58	9	42200	300
T59	10	>100000	-
T60	16	11000	800
INCB024360	93	64.6	0.1

-: Not detected; SD: Standard deviation for at least two runs.

Table 5. Inhibitory rates and IC_{50} (nM) values of the corresponding compounds against TDO at 10 μM

No.	% inhibition	TDO IC_{50}	SD	IDO IC_{50}(nM)	Selectivity[a]
T16	0	-	-	48	-
T23	38	-	-	152	-
T28	99.5	73.1	5.1	120	0.6
T44	76	1600	0.0	26	61.5
T51	100	684.3	2.6	207.9	3.3
T52	95	1200	100	289.5	4.2
T53	99	214.5	29.0	18	11.9
T54	98.5	321.5	3.5	22	14.6
T55	2	>100000	-	50300	-
T56	6	>100000	-	3300	-
T57	5	>100000	-	>100000	-
T58	1	>100000	-	42200	-
T59	1	>100000	-	>100000	-
T60	4	>100000	-	11000	-
680C91	92	376.5	2.8	-	-

[a] TDO IC_{50}/IDO1 IC_{50}; -: Not detected; SD：Standard deviation for at least two runs.

Table 6. T28, **T44** and **T53** suppresses kynurenine generation in vivo[a]

	plasma Kyn (μg/L)				
No.	0 h	SD	Min Concentration	SD	Max inhibition
T44	1639	560	818 (4h)	174	50.1%
T28	1476	183	902 (2h)	185	38.9%
T53	2920	1360	2030 (4h)	544	30.5%

[a] The average of three individual rat per treatment per time point.

Table 7. Cytotoxic activity of the promising compounds

No.	IDO1 IC_{50}(nM)	MTT (μM)			LDH(μM)	
		Hela	293T	MCF-7	Hela	293T
T16	48±5.6	16.73±1.50	>20	9.59±1.59	>40	>40
T23	151.8±10.1	-	-	-	>40	>40
T28	119.6±8.3	>20	>20	>20	>40	>40
T33	134±35.4	-	-	-	>40	>40
T44	26.2±1.2	>20	>20	>20	>40	>40
T45	29±5.7	>20	>20	>20	>40	>40
T47	18±11.3	>20	>20	>20	>40	>40
T48	233.7±14.3	-	-	-	>40	>40
T49	61±7.8	>20	>20	>20	>40	>40
T50	338±79.2	-	-	-	>40	>40
T51	207.9±3.6	-	-	-	>40	>40
T52	289.5±33.3	-	-	-	>40	>40
T53	18±4.9	4.63±0.45	10.1±0.78	2.77±0.70	>40	>40
T54	22±8.5	2.72±0.34	6.65±1.04	2.64±0.91	>40	>40
Doxorubicin	-	0.66±0.04	1.13±0.11	0.37±0.03	-	-

-: Not detected;

Highlights

- 60 naphthoquinone derivatives were synthesized and evaluated for IDO1/TDO inhibitory activity.
- **T47**, **T53**, **T44** were the most potent IDO1 inhibitors (IC_{50} 18, 18, 26 nM) with high selectivity against TDO.
- **T28** was identified as a potent dual IDO1/TDO inhibitor (IC_{50} 120/72 nM).
- A single, oral dose of **T44** decreased kynurenine levels in rat plasma by 50.1%.